Remote Sensing of Environment xxx (2013) xxx–xxx

Contents lists available at SciVerse ScienceDirect

Remote Sensing of Environment

journal homepage: www.elsevier.com/locate/rse

The assessment of optimal MERIS ocean colour products in the shelf waters of the KwaZulu-Natal Bight, South Africa

Marié E. Smith [a,*], Stewart Bernard [a,b], Sean O'Donoghue [c,1]

[a] Department of Oceanography, University of Cape Town, Rondebosch 7700, South Africa
[b] Earth Systems Earth Observation, Council for Scientific and Industrial Research, Centre for High Performance Computing, 15 Lower Hope Street, Rosebank 7700, South Africa
[c] School of Biological Sciences, Westville Campus, University of KwaZulu-Natal, Private Bag X54001, Durban 4000, South Africa

ARTICLE INFO

Article history:
Received 8 June 2012
Received in revised form 29 May 2013
Accepted 3 June 2013
Available online xxxx

Keywords:
Remote sensing
Ocean colour
MERIS
3rd reprocessing
Case 2 regional processor
KwaZulu-Natal Bight
South Africa

ABSTRACT

The KwaZulu-Natal Bight is a highly variable bio-optical environment, where waters over the shelf can change from the oligotrophic case 1 conditions of the Agulhas Current to the case 2 inshore environment influenced by upwelling and riverine influx. This study represents the first radiometric and biogeochemical validation to be performed in the KwaZulu-Natal Bight. The aim is to assess the performance of the Medium Resolution Imaging Spectrometer (MERIS) normalised water-leaving reflectance (ρ_w), aerosol and chlorophyll *a* (Chl-a) products from the 2nd and 3rd reprocessing as well as the case 2 Regional (C2R) processor. Confidence flags indicated that the ocean colour products from the 2nd reprocessing were not reliable over the sampling site during the study period. Standard MERIS ρ_w products from the 3rd reprocessing gave good returns from 490 to 560 nm, with absolute percentage difference (APD) of 10–16%, whilst underestimations in the red ranged from 124 to 215% compared to in situ data. Adjacency correction with the improved contrast between ocean and land (ICOL) processor leads to a decrease in APD. The C2R gave mostly low correlation coefficient values with a positive bias; APD ranged from 9 to 13% in the blue, whilst the poorest performing waveband was 620 nm with an APD of 67% compared to in situ data. The 3rd reprocessing with ICOL correction Ångström exponent showed the best correlation ($R^2 = 0.951$) with in situ data. The Chl-a product for case 1 waters from the 3rd reprocessing, Algal1, had the best agreement with in situ data, with a correlation coefficient of 0.796 and an APD of 54%. The Algal2 and C2R Chl-a products had low correlation coefficients and APD ranging from 72 to 103%. A dynamic per pixel classification technique for applying optimal MERIS Chl-a algorithms in the KwaZulu-Natal Bight or similar south-east African water types is described and evaluated in conjunction with the MERIS fluorescence line height product.

1. Introduction

Remotely-sensed ocean colour offers a unique means of studying the ocean, allowing the examination of biological and geophysical events such as river plumes (Dzwonkowski & Yan, 2005; Hu, Montgomery, Schmitt, & Muller-Karger, 2004; Molleri, deM Novo, & Kampel, 2010), eddies (Hirawake, Kudoh, Aoki, & Rintoul, 2003; Pegau, Boss, & Martinez, 2002) and algal blooms (Hu, Luerssen, Muller-Karger, Carder, & Heil, 2008; Pitcher, Bernard, & Ntuli, 2008; Ryan et al., 2009) over larger spatial and temporal scales than can be accomplished by conventional ship-based measurements. However, the successful application of ocean colour remote sensing products requires the use of atmospheric correction and in-water algorithms appropriate to the region under consideration.

Morel and Prieur (1977) originated the classification scheme of dividing the ocean into areas of case 1 and case 2 waters based on the ratio of pigment concentration to the scattering coefficient. These definitions were further developed (Gordon & Morel, 1983; Morel, 1988) so that the optical properties of case 1 waters were predominantly determined by phytoplankton and the coloured dissolved organic matter (CDOM) and detritus associated degradation products. Other waters were assumed to be case 2, where the optical properties could be influenced by various substances which do not necessarily co-vary with the phytoplankton concentration, e.g. mineral particles and CDOM. Discussions by Mobley, Stramski, Bissett, and Boss (2004) have since prompted a shift away from this classical bipartite approach, when they highlighted some of the instances where the classification scheme did not hold true (e.g. Balch, Kilpatrick, Holligan, & Fernandez, 1996; Boss & Zaneveld, 2003; Bricaud, Morel, & Prieur, 1981). A suggestion was to redesign the original definitions so that waters were case 1 if an optical quantity could be adequately predicted from the water column chlorophyll concentration; and case 2 if it could not. The relative simplicity of these idealised waters formed the basis of ocean colour chlorophyll retrieval algorithms,

* Corresponding author. Tel.: +27 731507061, +27 216505775 (work).
E-mail addresses: ocean.chiq@gmail.com (M.E. Smith), sbernard@csir.co.za (S. Bernard), Sean.O'Donoghue@durban.gov.za (S. O'Donoghue).
[1] Room 226, City Engineers Complex, 166 KE Masinga Road, Durban, 4000, South Africa.

0034-4257/$ – see front matter © 2013 Published by Elsevier Inc.
http://dx.doi.org/10.1016/j.rse.2013.06.009

where simple empirical (e.g. Bowers, Harker, Smith, & Tett, 2000; Bowers, Evans, Thomas, Ellis, & Williams, 2004; O'Reilly et al., 2000; Werdell et al., 2009) and semi-analytical (e.g. Morel & Antoine, 2007) algorithms could be successfully applied to case 1 waters. More complex algorithms such as non-linear optimization techniques (e.g. Hu, Lee, Muller-Karger, & Carder, 2003; Kutchinke, Gordon, & Franz, 2009; Maritorena, Siegel, & Peterson, 2002) and neural networks (e.g. Doerffer & Schiller, 2007, 2008a), which can take into account the inherent optical properties of the in-water constituents, are often required to obtain chlorophyll a (Chl-a) concentrations from case 2 waters.

The KwaZulu-Natal Bight on the east coast of South Africa is an example of a highly dynamic area where oligotrophic phytoplankton dominated case 1 waters can occur interchangeably with riverine influenced case 2 waters over a scale of tens of kilometres. Best practice application of ocean colour products in this bio-optically variable ecosystem ideally requires dynamic classification, i.e. algorithm selection on a per-pixel basis to ensure optimal algorithm selection across variable water types.

Data from the Medium Resolution Imaging Spectrometer (MERIS) were chosen for application in this area due to the convenient availability of standard (Doerffer & Schiller, 2007) as well as regional (Doerffer & Schiller, 2008a) case 2 products suited for use in coastal waters. A great deal of work has been done on validating MERIS products in a variety of bio-optical environments. Some of these have included coastal areas (Aiken et al., 2007; Cristina, Goela, Icely, Newton, & Fragoso, 2009; Gower & King, 2007; Park, Van Mol, & Ruddick, 2006; Schroeder, Schaale, & Fischer, 2007), open oceans and optically clear seas (Antoine et al., 2008; Cristina et al., 2009; Ohde, Siegel, & Gerth, 2007; Theis, Schmitt, Gehnke, Doerffer, & Bracher, 2008), lakes (Binding, Greenberg, Jerome, Bukata, & Letourneau, 2011; Gons, Auer, & Effler, 2008; Odermatt, Giardino, & Heege, 2010; Ruiz-Verdú et al., 2008), as well as partially enclosed seas that are heavily influenced by rivers and/or glaciers (Cui et al., 2010; Folkestad, Pettersson, & Durand, 2007; Kratzer, Brockmann, & Moore, 2008; Ohde et al., 2007; Sørensen, Aas, & Høkedal, 2007; Zibordi, Mélin, & Berthon, 2006). MERIS products have been used in various cases in Southern Africa. Aiken et al. (2007) undertook a validation study of MERIS standard products of reflectances and case 1 Chl-a in the southern Benguela on the west coast of South Africa. Matthews, Bernard, and Winter (2010) have also used MERIS full resolution data to monitor Zeekoevlei lake in Cape Town, South Africa. In addition, considerable research concerning MERIS utility for application in the Benguela upwelling system has taken place in South Africa (Bernard et al., 2006; Pitcher et al., 2008) and operational MERIS processing chains are in place at the Marine Remote Sensing Unit in Cape Town.

MERIS wavebands also are appropriately configured to detect the Chl-a fluorescence signal in the red (Babin, Morel, & Gentili, 1996; Xing, Kong, Cao, Zhang, & Tan, 2007). This fluorescence signal is specific to Chl-a, and can thus be unambiguously associated with phytoplankton. It is of potential use in case 2 waters, where the determination of Chl-a concentrations can be challenging if there is also influence from total suspended matter (TSM) and/or CDOM that is not related to changes in Chl-a. The signal can be represented by the fluorescence line height (FLH), the height of the fluorescence signal at 681 nm above a baseline formed by 665 and 709 nm. Chl-a fluorescence is usually a response of phytoplankton to environmental factors (e.g. light and nutrients) and thus the relationship between fluorescence and Chl-a can be highly variable (Babin et al., 1996). As a result it can be difficult to use quantitatively. However, it can still be used as a qualitative signal for the presence of phytoplankton in case 2 waters, particularly by examining the coherency between synoptic features in candidate algorithm and FLH products.

This study represents the first radiometric and bio-optical ocean colour product validation measurements to be performed in the waters of the KwaZulu-Natal Bight. The objective of this paper is to assess the MERIS level 2 reflectance products for nine bands, including 412.5, 442.5, 490, 510, 560, 620, 665, 681.25 and 708.75 nm (converted to remote sensing reflectance R_{rs} for comparison to in situ data) as well as the aerosol, case 1 and case 2 Chl-a products. This is the first step towards assessing the reliability of ocean colour products and allows the determination of error estimates.

Data from the MERIS 3rd reprocessing were released in 2011. This version includes updated case 1 and case 2 atmospheric correction and marine algorithms (Lerebourg & Bruniquel, 2011). Both the 2nd and the 3rd MERIS reprocessing data are evaluated in this paper.

Although the end of the Envisat mission was declared in May 2012, results from this study will be applicable to the next generation Ocean Land Colour Instrument (OLCI) onboard ESA satellite Sentinel-3 which is due for launch in 2013. OLCI is the replacement for MERIS and will have a similar waveband set-up, spectral sensitivity as well as processing algorithms for case 1 and case 2 waters.

2. Site description

The KwaZulu-Natal Bight is a distinct offset along the relatively smooth coastline, narrow continental shelf and steep slope of the east coast of South Africa. Along this 160 km of coastline the shelf extends up to 50 km offshore at its broadest point at the Thukela River mouth (Lutjeharms, Valentine, & Van Ballegooyen, 2000) with a slight continental slope compared to the surrounding coast. The Bight is flanked by the fast poleward flowing Agulhas Current on its oceanic boundary which follows the shelf break at the 200 m isobath, thus partially enclosing the waters of the KwaZulu-Natal Bight.

The Agulhas current controls the nutrient distribution over the majority of the Bight via various upwelling and retention processes, the most important of which is the topographically induced upwelling cell in the north of the Bight (Meyer, Lutjeharms, & de Villiers, 2002). These relatively high nutrient waters are subsequently transported southwards over the Bight at all depths (Lutjeharms et al., 2000) or occasionally advected downstream at the shoreward edge of the current (Meyer et al., 2002), and can therefore have a substantial influence on the phytoplankton productivity over the whole Bight (Carter & d'Aubrey, 1988; Carter & Schleyer, 1988). A number of estuarine inputs of freshwater and nutrients, the presence of a cyclonic eddy over the shelf, together with the upwelling in the north have resulted in the KwaZulu-Natal Bight being an important southern African nursery ground (Hutchings et al., 2002). The significant retention and concentration mechanisms that operate in the nearshore regions of the Bight lead to the Bight waters being more productive than the oligotrophic Agulhas current waters that are generally found in the surrounding coastal areas. Consequently, depending on the varying influence from the Agulhas current and riverine influxes, the bio-optical environment of the KwaZulu-Natal Bight can intermittently change between case 1 and case 2.

Data collection took place in the vicinity of the city of Durban, which is located near the Southern tip of the Bight. A sampling grid of four stations (see Fig. 1) was situated offshore from the Mgeni River mouth in an attempt to include possible case 2 conditions due to riverine influence. The sampling site was positioned further than 4 km from shore to avoid land-pixel flagging and adjacency effects (Takashima & Masuda, 2000) and in sufficiently deep water to avoid bottom reflectance (24–52 m). It is possible that the conditions of the sampling site may have been influenced to some degree by Durban Bay and the Durban harbour, and therefore may not be the best representation of the KwaZulu-Natal Bight in general. However, these data offer a feasible starting point given that there is no other information on the bio-optical conditions of the Bight.

Please cite this article as: Smith, M.E., et al., The assessment of optimal MERIS ocean colour products in the shelf waters of the KwaZulu-Natal Bight, South Africa, *Remote Sensing of Environment* (2013), http://dx.doi.org/10.1016/j.rse.2013.06.009

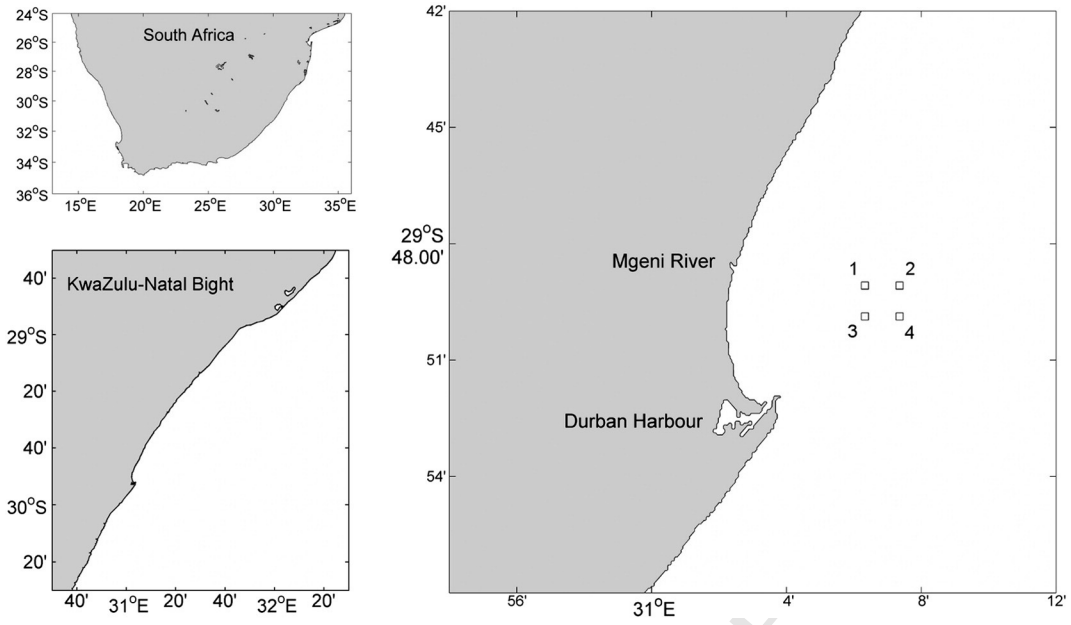

Fig. 1. The sampling grid and stations off Durban harbour and the Mgeni River mouth. The sampling site is located near the southern tip of the KwaZulu-Natal Bight.

3. Methods

3.1. In situ measurements

Data collection was completed in two stages, including a summer period from the 9th to 30th November 2009, and an autumn period from 27th April to the 14th May 2010. The aim was to firstly collect data during the summer rainy season, when the increase in riverine influx was most likely to produce a case 2 environment; and again at the start of the dry season, which could provide a "best-case" scenario, i.e. minimal case 2 influence. Unfortunately the lack of clear, cloudless days during the summer period resulted in the availability of only one potential match-up image, whilst there where at least four during the autumn period.

All measurements were taken within 2 h of the MERIS overpass which was generally around 9 am (GMT + 2 h). The sampling strategy at each station included radiometric measurements with coincident discrete water sampling collection at the surface and one other optically deeper depth. Deep water samples were collected at either 5 or 10 m depth (depending on the clarity of the water, as determined by Secchi depth) with Niskin bottles.

In-water radiometric measurements were made with a Hyperspectral Tethered Surface Radiometer Buoy (H-TSRB: Satlantic, Halifax, Canada), which measures upwelling near surface spectral radiance $L_u(z)$ at a nominal depth of 0.66 m, and above surface downwelling irradiance $E_d(0^+)$ in the range 400 to 800 nm at a 3.3 nm resolution with a spectral accuracy of 0.3 nm. Radiometric measurements were made for a duration of 3 min, whilst taking care to avoid any shading from the vessel during this time. Data were processed using the relevant proprietary software, Prosoft 6.3d (Satlantic: Halifax, Canada). A median $L_u(0.66)$ and $E_d(0^+)$ spectra were derived for each station from the whole sampling period, and subsequently resampled to a wavelength resolution of 5 nm.

In situ spectra were converted to remote sensing reflectance (R_{rs}) just above the sea surface for comparison with satellite data according to

$$R_{rs}\left(0^+,\lambda\right)=\frac{L_w(0^+)}{E_d(0^+)} \quad (1)$$

where $L_w(0^+)$ is the water-leaving radiance, which is determined by propagating $L_u(0.66)$ to just below the sea surface and subsequently correcting for the refraction and reflection from the air–water interface according to Snell's law:

$$L_w\left(0^+,\lambda\right)=\frac{1-r_F}{(n_w)^2}L_u(0.66)^{-K_{Lu}0.66} \quad (2)$$

where r_F is the Fresnel reflectance (≈0.02) according to Cox and Munk (1954), and n_w is the refractive index of water (≈1.33). K_{Lu} is the diffuse attenuation coefficient for upwelling radiance.

Since it is not directly measured, K_{Lu} was calculated with the use of the Ecolight 5 software (Sequoia Scientific, Inc.). Ecolight solves the azimuthally-averaged radiative transfer equation (RTE) to obtain azimuthally averaged radiances. This study did not require an azimuthally dependent radiative transfer equation and thus Ecolight was used instead of Hydrolight due to its computational efficiency. The Ecolight case 2 IOP model option was chosen, which is a generic 4-component IOP model that is recommended for general use. It offers flexibility and ease of use when defining component optical properties; the KwaZulu-Natal Bight waters are likely to be adequately described by these IOP models. The four components were pure water, pigmented particles (Chl-a), CDOM and mineral particles respectively.

For the pure water component the absorption coefficient was obtained from Pope and Fry (1997) whilst the scattering coefficient for pure sea water was computed from Morel (1974). The azimuthally averaged pure water phase function from Mobley (1994) was used.

The in vitro fluorometric Chl-a values from each station respectively were used as inputs to the model. The absorption by chlorophyll-bearing particles was taken from Prieur and Sathyendranath (1981) and Morel (1988), whilst the scattering was calculated with a power law model for near surface waters (Loisel & Morel, 1998). The Petzold "average-particle" phase function (as defined in Mobley et al., 1993) was used.

CDOM absorption values of between 0.02 and 0.1 m^{-1} were used as inputs to the model. The specific absorption a^* was calculated from an exponential decay function:

$$a^*(\lambda)=1^{[-0.014(\lambda-440)]} \quad (3)$$

whilst the azimuthally averaged isotropic phase function was used where CDOM covaries with Chl-a.

Mineral values of between 0.1 and 0.5 g m^{-3} were used as input. A wavelength-independent mass-specific scattering coefficient of zero was chosen for absorption, and calculated from the Prieur–Sathyenranath–Morel model (Morel, 1988; Prieur & Sathyendranath, 1981). A wavelength-independent mass-specific scattering coefficient of between 0.1 and 1 m^2 g^{-1} was chosen for scattering, which translated to a scattering coefficient of 0.05–0.1 m^{-1}. This is similar to the values described by Babin, Morel, Fournier-Sicre, Fell, and Stramski (2003) for the abovementioned inputs. The scattering was calculated using a power law model for near surface waters (Loisel & Morel, 1998), whilst the Petzold "average-particle" phase function (Mobley et al., 1993) was used.

The veracity of the modelling was tested by comparing the modelled L_u to the median $L_u(0.66)$ of the H-TSRB for each station. Some examples are provided in Fig. 2 that show a good agreement between the L_u spectra. If an appropriate modelled L_u was obtained, the corresponding modelled K_{Lu} was used to propagate the in situ $L_u(0.66)$ to just below the surface.

Aerosol Optical Thickness (AOT) was measured with a handheld Microtops II Sun Photometer Version 5.5 (Solarlight Co. 2003). It measures the AOT at five wavelengths in the visible and infrared spectrum at 440, 500, 675, 870 and 936 nm respectively. The handheld photometers are very sensitive to movement, and measurements are very difficult to perform from a small boat at sea. In order to improve the reliability of the measurements, the scans were performed on a stable platform in the harbour before and after the boat based sampling. All aerosol optical thickness measurements were taken between 9:20 and 11:30 am. Five AOT scans were made, and the scan with the lowest values was taken to be the true AOT. The Ångström exponent α was calculated from the AOT as follows (adapted from Ångström, 1964):

$$\alpha = -\left[ln\frac{\tau_a(\lambda_1)}{\tau_a(\lambda_2)}\right] \div \ln\frac{\lambda_1}{\lambda_2} \quad (4)$$

where τ_a is the AOT for adjacent Microtops wavelengths λ_1 and λ_2. Each pair of adjacent wavelengths from 440 to 870 nm was used to calculate α; subsequently a mean of the three exponents was used. $\tau_a(550)$ was calculated by linear interpolation between 500 and 675 nm for comparison with MERIS products.

Chl-a concentration was measured by fluorometric analysis (Holm-Hansen, Lorenzen, Holmes, & Strickland, 1965) with the use of a Turner Designs 10-AU. Fluorometric Chl-a samples were filtered through 25 mm Econofilt 0.7 μm (GF/F) filters subject to 10 mm mercury pressure. Sample volumes of 2 l were filtered (one surface, and one deeper optical depth per station). Filters were folded, placed in foil squares and frozen at −80 °C for analysis at a later stage. Ultimately, filtered sample papers were placed in polypropylene tubes with 9 ml acetone (90%), ground with a glass rod for 1 min and then frozen for 24 h to allow for pigment extraction. The test tubes were then centrifuged at 2500 rpm for 10 min to reduce turbidity, after which the supernatant was transferred to glass tubes to be read in the fluorometer. The samples were corrected for absorption by pheophytin pigments with the use of acidification.

The optically weighted Chl-a (C_f) was calculated for each available station from in situ data, in order to have a more accurate estimation for comparison with satellite retrieved values. Each station had a surface and one deeper measurement (at either 5 or 10 m), which could be used for the integration process. C_f was calculated using the following equation (Gordon & Clarke, 1980):

$$C_f = \frac{\int_0^{Z_{90}(\lambda)} C(z)f(z)dz}{\int_0^{Z_{90}(\lambda)} f(z)dz} \quad (5)$$

$f(z)$ is given by:

$$f(z) = \exp\left(-2\int_0^z K_d\left(\lambda, z'\right)dz'\right) \quad (6)$$

where $C(z)$ is the phytoplankton pigment concentration at depth z; K_d and Z_{90} are the vertical attenuation coefficient and the penetration depth respectively. The penetration depth was calculated as follows (Gordon & McCluney, 1975):

$$z_{90} = 1/K_d(\lambda) \quad (7)$$

K_d can be estimated from (Morel, 1988; Morel & Maritorena, 2001):

$$K_d = K_w(\lambda) + \chi_m[Chl]^e \quad (8)$$

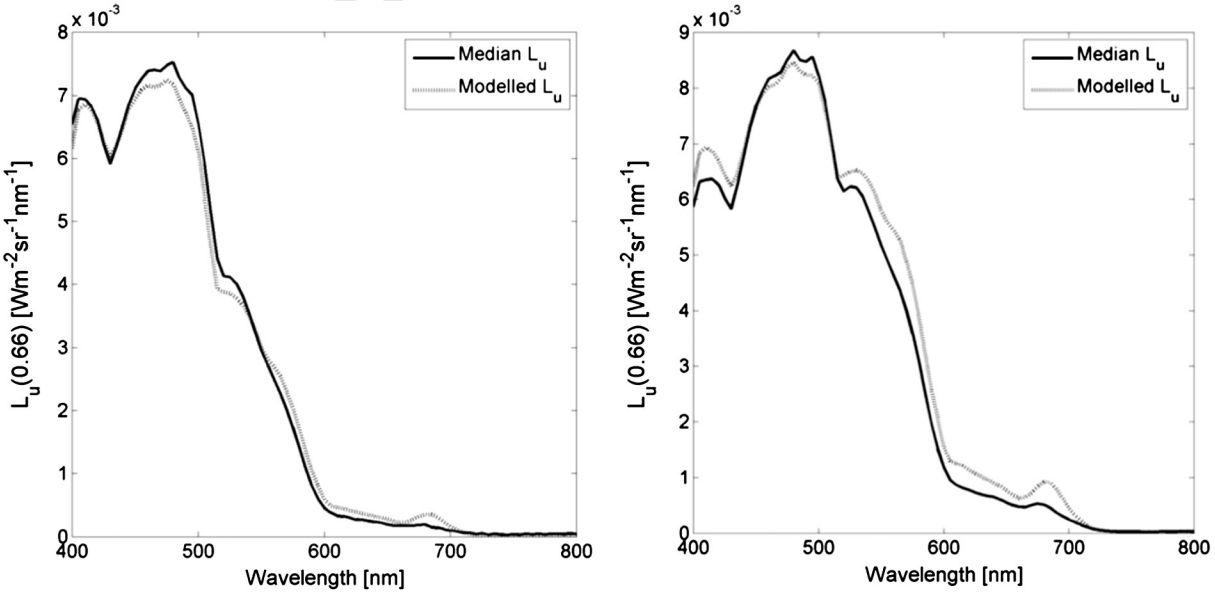

Fig. 2. Examples of the Satlantic median L_u spectra (measured at 0.66 m) compared to the modelled L_u output by Ecolight for 0.66 m.

where the term K_w is the attribution of pure water, and $\chi_m[Chl]^e$ is the term for all biogenic components; K_w, χ_m and e were obtained from Morel and Maritorena (2001).

Secchi depth was used as a proxy of water clarity and sediment loading, as well as an approximate indication of the upper optical depth when sampling. As a preliminary estimate Secchi depth of >15, 5–10 and <5 m would result in water collection at 10, 5, and 2 m respectively.

Backscattering profiles were performed at each station with the use of a HydroScat-2 (HOBI Labs 2004), which measures total backscattering at 420 nm and 700 nm and also fluorescence at 700 nm. Data were downloaded from the instrument in raw format, and converted to calibrated b_b units (Maffioni & Dana, 1997) with the HydroSoft v.2.7 (2004) software package for HOBI Labs Optical Oceanographic Instruments.

3.2. MERIS imagery

The data used were reduced resolution (1 km) MERIS level 1b and 2 data. Three types of MERIS products were compared: the 2nd reprocessing level 2 data which used the MERIS Ground Segment (MEGS) v7.4, the 3rd reprocessing (MEGS v8.0) level 2 data, and the level 2 data from the case 2 regional (C2R) processor which used the level 1b data from MEGS v8.0 as input. The product files were examined using the VISAT BEAM (v4.9.0.1) software package (Brockmann Consult). The pixels around the stations were inspected for quality flags before further analysis.

The improved contrast between ocean and land (ICOL) processor v2.7.4 (Santer, 2010) was used to account for adjacency effects. The adjacency effect can occur over coastal waters when photons from the land are reflected and scattered towards the sensor; this contrast between the relatively bright land surface and dark ocean may lead to erroneous values of top of atmosphere radiance, resulting in increased uncertainties in level 2 water-leaving reflectance. The ICOL processor is available as a BEAM plug-in, and was applied to level 1b data files before they were processed by either ODESA or the C2R processor. The level 2 water-leaving reflectance and chlorophyll products with and without ICOL correction were assessed.

MEGS v7.4 level 1b and 2 data were downloaded from the MERIS catalogue and inventory (MERCI) website. These level 2 data were processed with the "bright pixel" atmospheric correction or BPAC (Aiken & Moore, 2000) and subsequently by an Antoine and Morel (2005) type atmospheric correction. The marine algorithms included the OC4Me, a semi analytical model for case 1 waters (Morel et al., 2007), and a neural network for case 2 waters (Doerffer & Schiller, 2007). All output from this processor will henceforth be referred to as MEGS7.

Level 1b and 2 data from the MERIS 3rd reprocessing (Lerebourg & Bruniquel, 2011) were obtained from the Optical Data Processor for ESA (ODESA) online processor which used MEGS v8.0. ICOL corrected level 1b data were individually processed with the ODESA v1.2.4 software. The 3rd reprocessing includes revised algorithms for BPAC (Moore & Lavender, 2011), OC4Me (Morel & Antoine, 2011) and a new case 2 marine neural network, as well as an additional atmospheric neural network for the retrieval of case 2 products (Doerffer, 2011). All output from this processor will hereafter be referred to as MEGS8.

The MERIS case 2 regional (C2R) processor v1.5.1 (Doerffer & Schiller, 2008a) was applied to the MEGS v8.0 level 1b data as an alternative to the BPAC and case 2 marine algorithms. The C2R processor comes standard in the BEAM toolbox (v4.9.0.1) and employs a coupled ocean–atmosphere neural network for the atmospheric correction of the sensor received signal measured over case 2 coastal and inland waters (Doerffer & Schiller, 2008a, 2008b). Hereafter all level 2 products or their derivatives resulting from the case 2 regional processor will be referred to as C2R.

The FLH/MCI processor v1.6.102 was also applied to MEGS level 2 data in order to extract the required fluorescence line height products. This processor comes standard in the BEAM toolbox, and applies the following formula:

$$\mathrm{FLH} = L_F - \mathrm{k}^* \left[L_L + (L_R - L_L) \frac{\lambda_F - \lambda_L}{\lambda_R - \lambda_L} \right] \quad (9)$$

where L_F, L_L, L_R and λ_F, λ_L, λ_R are the radiances and wavelengths of the fluorescence band and the two baseline bands respectively, and k is a correction factor for the effect of thin clouds (k = 1.005). The formula is based upon the algorithm of Gower, Doerffer, and Borstad (1999).

All MERIS reflectance products are delivered as water-leaving reflectances (ρ_w). To maintain a standard and to make the satellite data comparable to the in situ radiometric data, the MERIS ρ_w data were converted to R_{rs} according to the following relationship described by Antoine and Morel (2005):

$$R_{rs} = \rho_w / \pi. \quad (10)$$

The MERIS bands are centred over the 412.5, 442.5, 490, 510, 560, 620, 665, 681.25 and 708.75 nm wavelengths. Since all Satlantic radiometric data were processed to the nearest 5 nm, the wavelengths of 410, 440, 490, 510, 560, 620, 665, 680 and 710 nm data were chosen respectively for comparisons between the in situ and satellite R_{rs}.

3.3. Strategy for matching in situ and satellite data

The following match-up criteria were used for comparing in situ data to MERIS products:

a) MERIS products were acquired from the same day as in situ observations.
b) In situ observations were taken within 2 h of MERIS overpass.
c) From visual examination in BEAM, it was determined that the pixels surrounding the sampling stations were very similar with regard to water-leaving reflectances and in-water constituent concentration. A 3 × 3 megapixel mean (the pixel closest to the sea-truthing station together with the eight adjacent pixels) and standard deviation were used to represent the MERIS data for each station. This extraction was performed for the reflectance data as well as the aerosol and Chl-a products.
d) For reflectance products: all MEGS pixels that were affected by sun glint and/or the PCD1_13 flag were excluded. Pixels that were affected by the "atmospheric correction out of range" flag and sun glint were excluded for C2R data.
e) For Chl-a products: pixels that were affected by sun glint and/or the PCD15 flag were excluded from the statistical calculations of Algal1, whilst the PCD17 (uncertain Algal2 product) and "invalid case 2 pixel" flags were used to screen Algal2 and C2R data respectively.
f) A station had to have more than 50% viable and/or cloud-free pixels in order to be used for further match-up analysis. A list of the available pixels and their flags can be seen in Table 1.

The days that had clear images for possible match-up analysis were the 25th of November 2009 and the 6th, 9th, 10th and 12th of May 2010.

Several statistical parameters were used to evaluate the satellite match-up results. The average absolute percentage difference (APD) was used to assess uncertainties, whilst the average relative percentage difference (RPD) was used to assess biases. Other indicators included the Root Mean Square error (RMSe) and the coefficient of determination (R^2). The parameters were calculated as follows:

$$APD = \frac{1}{N} \sum_{i=1}^{N} \frac{|y_i - x_i|}{x_i} \times 100\% \quad (11)$$

Please cite this article as: Smith, M.E., et al., The assessment of optimal MERIS ocean colour products in the shelf waters of the KwaZulu-Natal Bight, South Africa, *Remote Sensing of Environment* (2013), http://dx.doi.org/10.1016/j.rse.2013.06.009

Table 1
Confidence and glint flags from the MEGS7, MEGS8 and C2R processors for all stations.

Date	St	MEGS7	MEGS8	MEGS8 (with ICOL)	C2R
2009-11-25	1	Med glint[a], PCD1_13	Med glint, PCD1_13	Med glint	–
2009-11-25	2	Med glint, PCD1_13	Med glint, PCD1_13	Med glint	–
2009-11-25	3	Med glint, PCD1_13	Med glint, PCD1_13	Med glint	–
2009-11-25	4	Med glint, PCD1_13	Med glint, PCD1_13	Med glint	–
2012-05-06	1	PCD1_13, PCD15, PCD19	–	–	–
2012-05-06	2	PCD1_13	–	–	–
2012-05-06	3	PCD1_13	–	–	–
2012-05-06	1	PCD1_13, PCD15, PCD19	–	–	–
2012-05-09	1	PCD1_13, PCD15, PCD19	–	–	–
2012-05-09	2	PCD1_13, PCD15, PCD19	–	–	–
2012-05-09	3	PCD1_13, PCD15, PCD19	–	–	–
2012-05-09	4	PCD1_13, PCD15, PCD19	–	–	–
2012-05-10	1	PCD1_13, PCD15, PCD19	–	–	–
2012-05-10	2	PCD1_13, PCD15, PCD19	–	–	–
2012-05-10	3	PCD1_13, PCD15, PCD19	–	–	–
2012-05-10	4	PCD1_13, PCD15, PCD19	PCD1_13	PCD1_13	–
2012-05-12	1	PCD1_13, PCD15, PCD19	PCD1_13	–	–
2012-05-12	2	PCD1_13, PCD15, PCD19	–	–	–
2012-05-12	3	PCD1_13, PCD15, PCD19	PCD1_13, PCD15	PCD1_13, PCD15	Atcoor[b]
2012-05-12	4	PCD1_13, PCD15, PCD19	PCD1_13	–	–

[a] Medium glint.
[b] Atmospheric correction out of range.

$$RPD = \frac{1}{N}\sum_{i=1}^{N}\frac{y_i - x_i}{x_i} \times 100\% \quad (12)$$

$$RMSe = \sqrt{\frac{\sum_{i=1}^{N}(y_i - x_i)^2}{N}} \times 100\% \quad (13)$$

where y_i is the ith satellite-retrieved value, x_i is the ith in situ value and N is the number of data points. These statistics parameters were applied to R_{rs}, aerosol and Chl-a products.

4. Results

4.1. Satellite data validation

Out of the 15 days that in situ data were collected, there were five relatively cloud-free images with usable coverage over the sampling site. However, the presence of certain MERIS flags over sea-truthing stations led to the exclusion of some pixels. Table 1 showed that the most commonly occurring flags were the MERIS confidence or PCD flags. These PCD flags are a combination of other single criteria flags and offer a good synthesis for the various types of conditions that may affect the reliability of the data.

The PCD1_13 flag was raised for all the stations in the MEGS7 images. This is a confidence flag for all the reflectance values, and indicates that the atmospheric correction has failed in at least one of the bands (Brockmann, 2006). The flag is raised when triggered by one or a combination of other factors or flags: low sun angles; ice-haze flag (the measured radiance at the sensor is too high to be used in the inversion process, which can be caused by ice in the atmosphere or by very high optical thickness); out-of-aerosol database flag (the case 1 atmospheric correction algorithm could not find two aerosol models in its database which fit the measured signal in the near infrared); uncorrectable sun glint; and/or when reflectances in any of the bands from 1 to 13 are negative.

The PCD15 and PCD19 flags, which are the confidence flag for Algal1 and the confidence flag for the atmospheric Ångström coefficient and the aerosol optical thickness respectively, were also triggered over many of the pixels from MEGS7 images. The PCD15 flag can be raised due to one or a combination of factors, including atmospheric correction failure, difficulties with aerosol correction, uncorrected glint or whitecaps and/or high turbidity. The PCD19 flag can be raised due to atmospheric correction failure, glint or whitecaps, high yellow substance and/or when the retrieved aerosol model does not match the aerosol climatology.

Given that the PCD1_13 flag was often raised in conjunction with the PCD15 and PCD19 flags for MEGS7 images, it may be assumed that the cause of flagging was most likely due to atmospheric correction failure as a result of difficulties with the aerosol correction and/or model selection. This would also indicate that the level 2 data corresponding to those pixels would most likely contain serious errors and should not be trusted. Consequently the MEGS7 data are only included in further results as an indication of the level of improvement obtained by the other processing methods.

The amount of flags decreased when images were processed by MEGS8 instead of MEGS7, and even less pixels were flagged when data were corrected for adjacency effects before level 2 processing. Images processed by the C2R processor had the least amount of flagged pixels. Ultimately there were 12 stations which could be used for comparison between in situ data and all versions of MERIS processing. The direct comparison of R_{rs} spectra can be seen in Fig. 3.

The MEGS spectra maintained a very similar spectral shape to in situ data between 490 and 710 nm, showing good agreement in the green, with some underestimation in the red. MEGS data without adjacency correction had a greater tendency to underestimate compared to where ICOL had been applied. The most noticeable divergence in spectral shape occurs at 412.5 and 442.5 nm. Previous studies have also found large amounts of noise in the 412.5 nm MERIS band (e.g. Antoine et al., 2008; Cristina et al., 2009; Park et al., 2006). The outputs from the MEGS algorithm often showed small amounts of negative reflectance values in the red and NIR regions.

C2R obtained similar values to in situ in the blue; it maintained a very constant spectral shape, but mostly over-estimated between 490 and 710 nm. Chlorophyll-related spectral features (e.g. fluorescence) were not as prominent as those produced by MEGS, since the C2R atmospheric correction procedure does not include inelastic scattering processes (Binding et al., 2011). The C2R spectra where ICOL had been applied showed almost identical results to those without adjacency correction; consequently only the ICOL corrected spectra are shown in Fig. 3.

Please cite this article as: Smith, M.E., et al., The assessment of optimal MERIS ocean colour products in the shelf waters of the KwaZulu-Natal Bight, South Africa, *Remote Sensing of Environment* (2013), http://dx.doi.org/10.1016/j.rse.2013.06.009

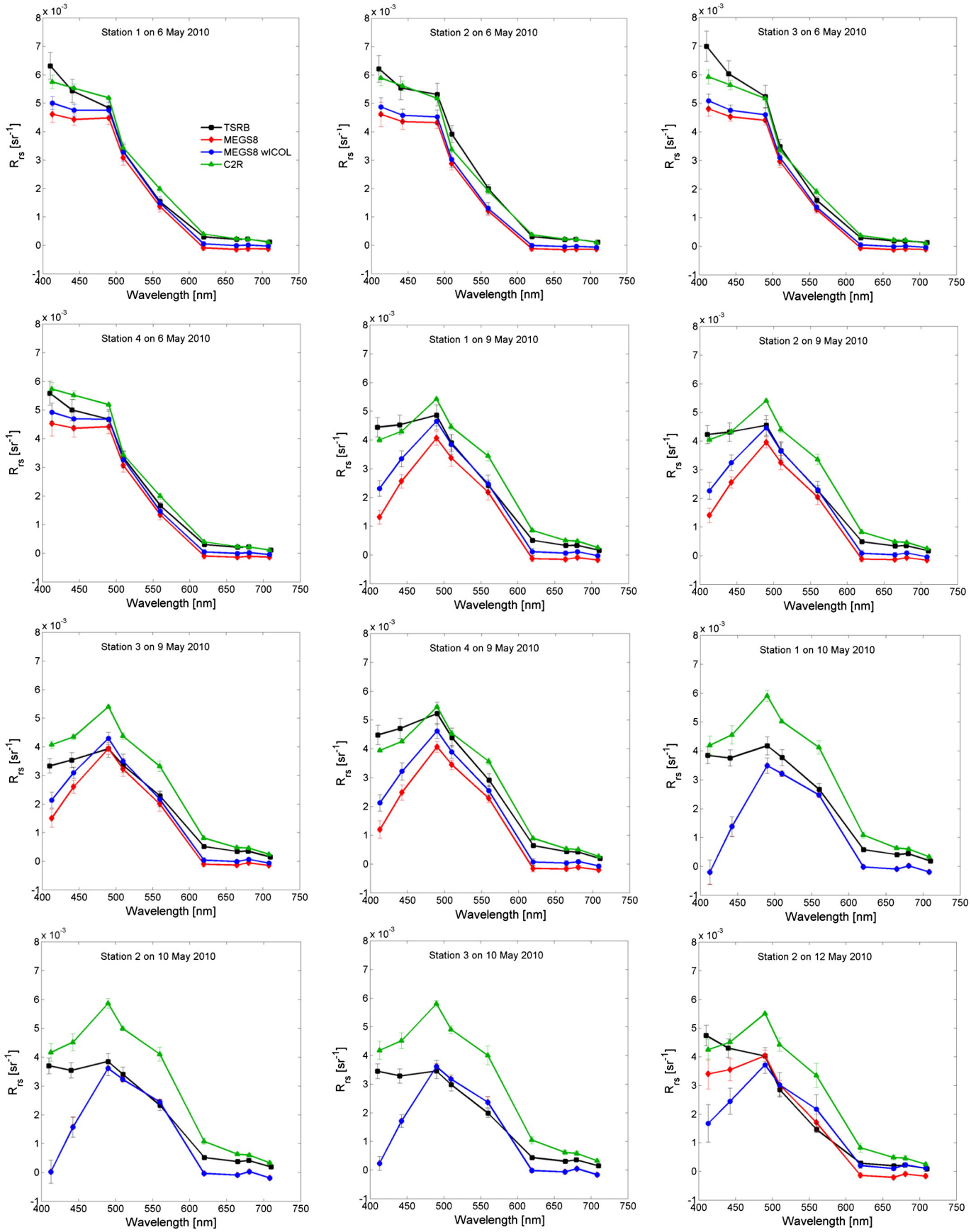

Fig. 3. The R_{rs} spectra of the in situ TSRB data (black), MEGS8 (red), MEGS8 with ICOL (blue) and C2R (green) processors respectively on the 12 days that data were available for each of them. C2R with and without ICOL processing were almost identical and thus only one line was included. The TSRB points represent the median value and the error bars indicate the quadrature sum uncertainty, whilst for the MERIS products the points and error bars are the 9 pixel mean and standard deviation respectively. The legend in the first image applies to all the images. (For interpretation of the references to colour in this figure legend, the reader is referred to the web version of this article.)

Please cite this article as: Smith, M.E., et al., The assessment of optimal MERIS ocean colour products in the shelf waters of the KwaZulu-Natal Bight, South Africa, *Remote Sensing of Environment* (2013), http://dx.doi.org/10.1016/j.rse.2013.06.009

The statistics of comparisons between in situ and MERIS R_{rs} products for discrete wavelengths are given in Table 2. The bias is negative at most wavelengths for the MEGS8 processor, confirming the tendency of MEGS to underestimate R_{rs} on average. Similar results were obtained for MERIS data in the case 1 waters of the Atlantic (Theis et al., 2008) and at inshore stations off the coast of Portugal (Cristina et al., 2009). MEGS8 R_{rs} data showed smaller bias and uncertainties at all wavelengths following the application of ICOL, with the most improvement noticeable in the red. The best performing match-ups for the MEGS8 processor were the wavelength bands between 490 and 560 nm where adjacency correction was applied, showing higher coefficients of determination and lower uncertainties. Previous studies have also found that these yield higher accuracy than other bands (Antoine et al., 2008; Cui et al., 2010; Ohde et al., 2007; Sørensen et al., 2007; Zibordi et al., 2006). The MEGS processor showed the poorest performance in the red, with the application of ICOL showing smaller RPDs, but lower R^2 values. Cristina et al. (2009) had similar results at their inshore station, with bias values from −75.4 to −91.5% in the red, whilst Antoine et al. (2008) also found the longer wavelengths to perform worse than other bands.

The C2R algorithms showed a mostly positive bias, with the best performance in the blue. Although the C2R showed predominantly lower RPD and APD values than the MEGS processor in the longer wavelengths, the results showed very little correlation to in situ values; this is perhaps due to the relatively small range of bio-optical conditions presented. The application of ICOL had almost no effect on the C2R R_{rs} data.

Table 2
Statistics of comparison between in situ measurements and MERIS R_{rs} products from MEGS8 and C2R processors respectively (MEGS8 N = 14, C2R N = 19).

Band [nm]	MEGS7 (without ICOL)			
	R^2	RPD %	APD %	RMS
410	*0.387*	*−25*	*36*	*0.160*
440	*0.317*	*−11*	*19*	*0.091*
490	*0.001*	*6*	*12*	*0.067*
510	*0.016*	*7*	*14*	*0.064*
560	*0.381*	*9*	*21*	*0.052*
620	*0.091*	*−91*	*91*	*0.042*
665	*0.119*	*−120*	*120*	*0.036*
680	*0.287*	*−86*	*86*	*0.028*
710	*0.217*	*−154*	*154*	*0.023*

[nm]	MEGS8 (without ICOL)				MEGS8 (with ICOL)			
	R^2	RPD %	APD %	RMSe	R^2	RPD %	APD %	RMSe
410	0.830	−58	58	0.267	0.793	−53	53	0.242
440	0.776	−35	35	0.159	0.803	−31	31	0.138
490	0.557	−10	10	0.063	0.677	−5	7	0.040
510	0.214	−9	11	0.052	0.370	−4	6	0.034
560	0.574	−9	16	0.038	0.512	1	14	0.034
620	0.004	−124	124	0.053	0.000	−81	81	0.039
665	0.095	−152	152	0.044	0.001	−96	96	0.031
680	0.445	−128	128	0.038	0.040	−73	73	0.026
710	0.531	−215	215	0.031	0.204	−129	131	0.022

Band [nm]	C2R (without ICOL)				C2R (with ICOL)			
	R^2	RPD %	APD %	RMSe	R^2	RPD %	APD %	RMSe
410	0.832	1	9	0.049	0.832	2	9	0.047
440	0.633	10	13	0.061	0.633	11	13	0.061
490	0.096	21	22	0.118	0.095	21	22	0.117
510	0.022	15	25	0.105	0.037	15	25	0.106
560	0.004	34	46	0.119	0.000	33	47	0.120
620	0.051	58	66	0.035	0.032	57	67	0.036
665	0.071	34	47	0.018	0.049	33	48	0.018
680	0.065	20	37	0.016	0.046	19	38	0.017
710	0.015	40	55	0.012	0.006	39	56	0.010

Table 3
Statistics of comparisons between in situ measurements and MERIS level 2 chlorophyll products. (The mean and standard deviations of the in situ Chl-a concentrations can be seen in Table 7.)

	R^2	RPD %	APD %	N
Algal1 (MEGS7)	–	–	–	2
Algal1 (MEGS8)	0.796	50	54	15
Algal1 (MEGS8 w ICOL)	0.867	67	73	15
Algal2 (MEGS7)	0.096	46	103	18
Algal2 (MEGS8)	0.123	69	72	18
Algal2 (MEGS8 w ICOL)	0.173	69	73	18
C2R Chl (MEGS8)	0.374	95	98	18
C2R Chl (MEGS8 w ICOL)	0.396	92	96	18

The statistics of comparisons between in situ and MERIS chlorophyll products are given in Table 3. The Algal1 product from MEGS7 could not be used for comparison since only two data points were available. The Algal1 product from the MEGS8 processor with adjacency correction showed the best correlation with in situ data, whilst MEGS8 without ICOL had the lowest uncertainty. Antoine et al. (2008) found similar correlations between in situ data and Algal1. Although the application of ICOL showed slightly increased coefficients of determinations for all processors, it did not significantly change the RPD and APD from Algal2 and C2R Chl-a products, and results were still noisy when compared to in situ measurements. This study corresponds to previous findings (Binding et al., 2011; Koponen et al., 2008; Odermatt et al., 2010) showing that the application of ICOL generally improves the agreement between MERIS and in situ spectral reflectance, but does not significantly improve estimates of water constituents.

The statistics of Microtops measurements can be seen in Table 4. These data include non-overpass days and are mostly from May 2010, with only one measurement taken on 25 November 2009. The $\tau_a(500)$ varied between 0.134 and 0.321; these are higher values compared with oceanic areas that are generally characterised by $\tau_a(500)$ of less than 0.10 (Smirnov et al., 2011). These relatively high $\tau_a(500)$ values could indicate that, in addition to maritime aerosols, other aerosols could have been influencing the atmosphere in the southern parts of the KwaZulu-Natal Bight, possibly originating from the urban and industrial areas of Durban. The relatively high mean Ångström exponent of also 1.142 indicates that there were fine particles present in the atmospheric column (Smirnov et al., 2011).

There was good agreement between the Microtops and MEGS8 Ångström exponents (Table 6), with relatively low bias and uncertainties. ICOL slightly improved these results. The C2R processor produced lower Ångström exponents than MEGS8, often showing negative slopes (Table 5). This lead to large amounts of scatter and underestimation of up to 71% compared to Microtops data. Both MEGS8 and C2R slightly underestimated $\tau_a(500)$ and had similar uncertainties. Although the C2R showed the best correlation with Microtops data, all processors showed a large amount of scatter.

The statistics of in situ measurements taken over the two sampling seasons can be seen in Table 7. Chl-a concentrations were slightly higher in summer compared to autumn. Secchi depth values were relatively high, ranging from 6 to 11 m in summer and 7 to 30 m in autumn. These coincided with reasonably low mean b_b values.

Table 4
Statistics of Microtops measurements (including non-overpass days).

	Mean ± st. dev.	Median	Max	Min	N
α	1.142 ± 0.205	1.089	1.470	0.913	9
$\tau_a(500)$	0.224 ± 0.076	0.191	0.321	0.134	9

Table 5
Statistics of MERIS level 2 Ångström exponent and $\tau_a(550)$ products.

	Mean ± st. dev.	Median	Max	Min	N
α					
MEGS8	1.12 ± 0.41	1.490	1.57	0.52	12
MEGS8 (wICOL)	1.12 ± 0.39	1.27	1.46	0.30	12
C2R	0.37 ± 0.29	0.31	0.68	-0.14	19
C2R (wICOL)	0.38 ± 0.37	0.38	0.80	-0.31	19
$\tau_a(550)$					
MEGS8	0.154 ± 0.036	0.144	0.247	0.115	12
MEGS8 (wICOL)	0.145 ± 0.038	0.131	0.252	0.115	12
C2R	0.187 ± 0.075	0.152	0.305	0.107	19
C2R (wICOL)	0.174 ± 0.067	0.145	0.293	0.107	19

Table 7
Statistics of in situ measurements.

	Mean ± st. dev.	Median	Max	Min	N
Summer					
Chl-a (mg m^{-3})	1.05 ± 0.46	0.89	1.77	0.38	23
Secchi (m)	8.2 ± 1.1	8	11	6	14
b_b420 (m^{-1})	0.0092 ± 0.0010	0.009	0.0124	0.0074	921
Autumn					
Chl-a (mg m^{-3})	0.35 ± 0.12	0.34	0.64	0.09	72
Secchi (m)	15.3 ± 4.3	16	30	7	40
b_b420 (m^{-1})	0.0073 ± 0.0033	0.0065	0.0252	0.0040	6303

5. Discussion

5.1. Assessment of the bio-optical conditions

Chl-a concentrations during the two sampling periods were relatively elevated when compared to previous measurements made in the area. Meyer et al. (2002) found that the Chl-a concentrations over the southern parts of the Bight were less than 0.1 mg m^{-3}, whilst the central parts ranged between 0.1 and 0.5 mg m^{-3}. The comparative increase in Chl-a concentrations recorded during this study (0.09–1.77 mg m^{-3}), could indicate some mechanism of nutrient enrichment during these times.

Although reliable in situ data relevant to non-phytoplankon constituents were not available, it was still possible to make some inferences. Typical oceanic salinity values indicated no presence of riverine influence during the two research periods. Although there were no TSM data to support the validation, b_b values were similar to that described for case 1 waters (Babin et al., 2003); this also coincided with relatively high Secchi depth values (from 6 to 30 m). Although the derivation of IOP values from the measurement of Secchi depth is not always accurate, it is a still a useful qualitative measurement as there is a relationship between the depth of disappearance of the Secchi disc and the average amount of organic and inorganic materials along the path of sight down the water column (Preisendorfer, 1986).

Further evidence for the ranges of the water constituents were obtained when Ecolight was used to model the propagation of $L_u(0.66)$ through the water column and the air–sea interface. Input values of CDOM between 0.02 and 0.05 m^{-1}, and mineral values between 0.1 and 0.5 g m^{-3} were required for the correct simulation of the in situ L_u spectra. It would thus be prudent to assume that the in situ values of these constituents could fall in the ranges discussed above during the two sampling periods. It could therefore be concluded that the bio-optical environment consisted of case 1 type waters.

Table 6
Statistics of comparisons between Microtops and MERIS level 2 Ångström exponent products as well as Microtops interpolated $\tau_a(550)$ measurements and MERIS $\tau_a(550)$ products respectively.

	R^2	RPD %	APD %	RMSe %	N
α					
MEGS8	0.903	9	19	22.6	12
MEGS8 w ICOL	0.951	−2	14	15.8	12
C2R	0.524	−69	69	72.9	19
C2R w ICOL	0.630	−71	71	72.7	19
$\tau_a(550)$					
MEGS8	0.266	−10	18	3.5	12
MEGS8 w ICOL	0.373	−15	19	3.9	12
C2R	0.657	−4	21	5.0	19
C2R w ICOL	0.574	−10	22	4.8	19

5.2. Algorithm constraints and applicability

In order to facilitate optimal regional ocean colour product usage, it is important to be aware of the strengths, weaknesses and validity range of the atmospheric and water algorithms in order to make an informed decision with regard to the algorithm application approach.

The MERIS case 1 atmospheric correction, for instance, assumes that the aerosol models that are used represent good estimates of the actual aerosols over the ocean (Antoine & Morel, 2011). This atmospheric correction also cannot produce correct results over case 2 waters and is thus implemented after the bright pixel atmospheric correction in the ocean atmospheric correction chain; this step helps to identify and resolve any residual signal in the near infrared (e.g. backscattering from sediments or coccoliths) in order to avoid failure of the case 1 algorithm.

The bright pixel atmospheric correction has difficulties with adjacency effects, particularly in low turbidity waters (Lerebourg & Bruniquel, 2011). This could be improved by adjacency correction, as can be seen in Table 2 where the application of ICOL leads to slightly lower bias and uncertainties in the MEGS8 R_{rs}.

The C2R atmospheric NN avoids extrapolation from the NIR bands, and thus prevents the production of negative reflectance. The atmospheric correction is not independent of the water model, since water-leaving reflectances are produced using a forward radiative transfer model which incorporates the bio-optical model (Doerffer & Schiller, 2008a). For input into the marine algorithm, values of water-leaving reflectance outside of the input minimum or maximum are replaced by the corresponding minimum or maximum values (Doerffer & Schiller, 2008b). By its nature the C2R atmospheric correction is therefore more constrained than the MEGS processors.

The MERIS case 1 chlorophyll algorithm or OC4Me has a tendency to overestimate in case 2 waters (Morel & Antoine, 2011), and would also produce wrong results in areas that are contaminated by sun glint. It can be assumed that the Algal1 product would be reliable, unless the PCD15 flag is triggered; however, it would be prudent to first examine the Algal1 data in sun glint affected areas before accepting the values as correct.

The new MERIS case 2 chlorophyll product, Algal2, is the output of a coupled NN based on the case 2 regional type approach. The chlorophyll retrievals from the NN do not go below 0.04 (Lerebourg & Bruniquel, 2011); however the minimum in situ chlorophyll value was 0.09 mg m^{-3} and thus falls within the training ranges. A problem with these case 2 products are that the confidence flags with regard to these products (PCD16 and PCD17) have not yet been properly adjusted. Bourg et al. (2012) recommend the exclusion of the case 2 products when any of the glint flags are raised, the case2_s flag is not raised and/or the TSM is higher than 20 mg L^{-1}.

The outputs of the C2R neural network are inherent optical properties. The default chlorophyll product for the C2R comes from an empirical relationship with the phytoplankton pigment absorption at 443 nm. This relationship was designed for the North Sea and might not be applicable in all waters.

Please cite this article as: Smith, M.E., et al., The assessment of optimal MERIS ocean colour products in the shelf waters of the KwaZulu-Natal Bight, South Africa, *Remote Sensing of Environment* (2013), http://dx.doi.org/10.1016/j.rse.2013.06.009

5.3. Algorithm performance with regard to atmospheric correction

Various negative ρ_w values were retrieved in the red and NIR by the MEGS8 processor. For the MEGS7 data, this invariably triggered the confidence flag PCD1_13, which is raised when there are negative reflectance values in any of the 13 wavebands. A negative tolerance threshold has been introduced in the 3rd reprocessing, since a slightly negative reflectance in long wavelengths can be regarded as noise around a very small signal (Lerebourg & Bruniquel, 2011). This partially explains the large bias at longer wavelengths for the MEGS processors.

For the MEGS7 data, the PCD15 and PCD19 flags were often raised over the sampling site pixels. Since neither the case 2 sediment flag nor the various causal flags for PCD1_13 were raised simultaneously, it is more likely that the confidence flags were triggered by a problem with the atmospheric correction or the incorrect retrieval of the aerosol model. These flags are mostly absent in the MEGS8 data, suggesting that the revised atmospheric correction algorithm over case 1 waters (Morel & Antoine, 2011) have addressed these matters.

The in situ derived reflectance was relatively high in the blue, indicating low CDOM absorption (Morel & Prieur, 1977). However, the R_{rs} from the MEGS processors were quite noisy for wavelengths in the blue (412 and 443 nm). Low correlation in the blue bands has previously been attributed to extrapolation error in the aerosol reflectance (Park et al., 2006) and also to underperformance of the atmospheric correction process (Antoine et al., 2008; Cristina et al., 2009). The MEGS processor showed a tendency to underestimate ρ_w, which Theis et al. (2008) considered to be due to possible overestimation of the atmospheric correction. In the 3rd reprocessing, although all pixels go through the BPAC screening, the BPAC flag is only raised if the atmospheric correction was applied successfully. For the MEGS8 data, BPAC was never successfully applied over the sampling site pixels, and thus the residual marine signal in the NIR was set to that of pure seawater (Lerebourg & Bruniquel, 2011). This could potentially lead to an underestimation of ρ_w in shorter wavelengths.

The C2R (Doerffer & Schiller, 2006, 2008a) overestimated at most bands, but showed smaller bias and uncertainty values compared to the MEGS processors in the blue and red. The nature of the C2R atmospheric correction was discussed in Section 5.2; the result is a robust algorithm, with the disadvantage of a potentially over-constrained R_{rs} formulation that exhibits little cohesion with in situ data.

In general the AOT and Ångström exponent provides information about the aerosol loading and the aerosol size (type) respectively (Toledano et al., 2007). Although both the MEGS8 and C2R processors showed poor correlation with Microtops AOT at 550 nm, the relatively small errors indicate that both processors provided a good estimate of the aerosol loading of the atmosphere. The high R^2 and relatively low bias and uncertainty of the MEGS8 Ångström exponent show that the aerosol models provided a good estimate of the aerosol types present. Even if the exact aerosol type or distributions have not been recorded, the lookup tables used by the MERIS case 1 atmospheric correction scheme can usually still represent the features of aerosol spectral dependencies with sufficient accuracy to enable the atmospheric correction (Antoine & Morel, 2011).

5.4. Uncertainties in the determination of R_{rs} for the H-TSRB

Some thought has to be given to the various sources of uncertainty for the in situ derived R_{rs}. These are generally considered as percentages of the processed R_{rs} value. The cumulative uncertainty in $L_u(0^-)$ is estimated to be about 5% when carefully performing the measurements with well-calibrated instruments (Antoine et al., 2006), although this value included the estimation of $L_u(0^-)$ with the use of K_{Lu} as well as a bidirectionality uncertainty (Antoine et al., 2006). Zibordi, Berthon, Mélin, and D'Alimonte (2011) found that this value was relatively smaller at 2.8%. For the purposes of this study a $L_u(0^-)$ uncertainty of 3% was used. The use of K_{Lu} for the calculation of $L_u(0^-)$ may introduce some errors; therefore an uncertainly of 2.2% was assumed (Zibordi et al., 2011). Zibordi and Voss (2010) suggested that calibration uncertainty for irradiance could vary from 1.1 to 3.4%. For the purpose of this study an estimate of 3.1% was assumed for E_d. The self-shading percentage error of the TSRB was estimated using look-up tables from Leathers, Downes, and Mobley (2001) and was found to be approximately 2%. However, previous studies suggests that this error may be larger in the red (Zibordi et al., 2011); consequently a value of 2.8% was assumed for all wavelengths. There can also be a discrepancy in the spatial scale between the in situ sample of a few litres and the satellite pixel which represents approximately 1 km^2 of ocean (Holm-Hansen et al., 2004). Conventional water sampling methods assume that phytoplankton (and other water constituents) are uniformly distributed in the top mixed layer of the water column (Kutser, 2004); this assumption could lead to large errors in satellite retrievals when patchiness of algal blooms occurs. However, the waters of the Bight are generally considered to be well-mixed (Lutjeharms et al., 2000), and thus an uncertainty of 2% was used to account for the scale difference with the satellite match-ups. Possible errors may also be introduced due to the tilt and roll of the instrument; consequently a 4.5% uncertainty was assumed to account for these geometric effects (Zibordi et al., 2011).

The quadrature sum for all the abovementioned uncertainties which could be associated with the derivation of R_{rs} was approximately 7.5%. This is similar to estimates made by Antoine et al. (2008) for the BOUSSOLE buoy, where an uncertainty budget of 6% was obtained for water-leaving radiance. Zibordi et al. (2011) also found quadature sum values of between 6.4 and 7.9% for the Tethered Attenuation Chain Colour Sensors (TACCS) buoys (Satlantic Inc.).

5.5. Algorithm performance with regard to chlorophyll products

The Algal1 product showed the best performance in the case 1 type bio-optical environment of the sampling period, with the highest coefficient of determination and slightly lower uncertainties. This is not surprising since the algorithm utilizes the best performing wavebands from the MEGS processor. Previous studies have also shown Algal1 to have fairly low variability and a tendency to predominantly overestimate at low concentration ranges (Antoine et al., 2008; Gower & King, 2007; Ohde et al., 2007).

The Algal2 products generally had higher uncertainties and more scatter than Algal1 products. Algal2 has been known to be noisier in case 1 waters (Doerffer & Schiller, 2007) and the variability in the performance of the Algal2 product has been observed in numerous other investigations (Ambarwulan, Mannaerts, van der Woerd, & Salama, 2010; Folkestad et al., 2007; Ohde et al., 2007; Sørensen et al., 2007). The MEGS8 Algal2 product has also been shown to have low correlation coefficients in relatively clear waters (Bourg et al., 2012). The case 2 branch of the 3rd reprocessing includes the atmospheric correction that was developed in the C2R processor which provides inputs of water-leaving radiance to the marine neural network (Lerebourg & Bruniquel, 2011); this new set-up could result in a reduction of noise. There is an improvement in the coefficient of determination between the MEGS7 and MEGS8 Algal2 products, with a decrease in uncertainty; however, in light of the recommendations listed in Section 5.2, the MEGS8 Algal2 results may not be very reliable since the case2_s flag was never raised (Bourg et al., 2012).

The C2R constantly overestimated Chl-a concentration; this is similar to results from Binding et al. (2011) where Chl-a concentrations below 20 mg m^{-3} were overestimated. C2R Chl-a products could be improved for the KwaZulu-Natal Bight by generating local IOP conversion factors for the region, based on further in situ chlorophyll and IOP data collection. These conversion factors can be edited and applied manually in the C2R processor in BEAM.

Please cite this article as: Smith, M.E., et al., The assessment of optimal MERIS ocean colour products in the shelf waters of the KwaZulu-Natal Bight, South Africa, *Remote Sensing of Environment* (2013), http://dx.doi.org/10.1016/j.rse.2013.06.009

The possible sources of error, which can be attributed to the methods used to collect the in situ Chl-a data, should be considered. The fluorometric method for determining Chl-a has been shown to produce underestimations of 30% along the continental margin of the northwestern Gulf of Mexico (Bianchi, Lambert, & Biggs, 1995), other studies have shown ranges from −68 to +53% at individual stations (Trees, Kennicutt, & Brooks, 1985). For the purposes of this study an error estimate of 50% was assumed for the fluorometric determination of Chl-a. Gordon (1992) estimated that the error introduced with the use of the optically-weighted Chl-a method should be less than 3% where the maximum stratification is 0.43 mg m^{-3} per metre and the particle and absorption coefficients covary with C_f. Errors could be larger when b_b changes with depth, but this is not applicable to this study. Thus a 3% error was assumed. The combined effects of a fluorometric determination error of 50% and a 3% uncertainty from the use of the optically weighted Chl-a method, equated to a quadrature sum error of 50.1%.

5.6. Switching algorithm

The location of the KwaZulu-Natal Bight relative to the Agulhas Current, in addition to changeable riverine influxes, creates an inherently variable bio-optical setting. Although case 1 type conditions might dominate over large spatial and temporal scales in the Bight, coastal areas can variably include case 2 waters, where retention mechanisms and occasional flood events could facilitate increases in the amounts of fluvial sediments and CDOM in surface waters. Successful regional algorithm application across the entire system requires ocean colour algorithms that can distinguish between potential case 1 and case 2 environments, and apply the appropriate algorithms to these distinctive water masses whilst switching seamlessly between them.

The environmental conditions presented during this study provided a case 1 environment, where it was shown that the Algal1 product from the 3rd reprocessing gives good results. However, the inherent design of many case 1 algorithms that use the peak reflectance in the blue and green spectral regions, results in failure in sediment and/or CDOM dominated waters due to enhanced scattering and absorption of light in these spectral regions (e.g. Blondeau-Patissier, Tilstone, Martinez-Vicente, & Moore, 2004; Darecki & Stramski, 2004; Morel & Antoine, 2011).

To date there have been few studies assessing the performance of the new case 2 branch of the 3rd reprocessing in case 2 waters, and thus there is little precedent for assessing the possible performance of these products, particularly Algal2, in the KwaZulu-Natal Bight. However, the C2R chlorophyll product has been shown to work well in the tropical coastal waters of Indonesia (Ambarwulan et al., 2010); this area included bio-optical conditions ranging from turbid estuarine to open ocean shelf-edge reef environments, which encompasses conditions similar to those expected during a flood or heavily riverine influenced event in the KwaZulu-Natal Bight. It is thus safe to assume that the corresponding C2R product (from MEGS8 level 1b data) would be a good substitute for Algal1 in coastal case 2 waters of the KwaZulu-Natal Bight.

A pragmatic solution for regional ocean colour application in the KwaZulu-Natal Bight is a simple switching algorithm for chlorophyll determination with the use of existing MERIS algorithms. The switching algorithm functions by applying a default “background” product, which can be exchanged for an “overlay” product on a pixel-by-pixel basis. A pixel is only switched when “triggered” by a predetermined flag. Since the waters adjacent to the KwaZulu-Natal Bight are known to be relatively clear and have a strong influence on the waters of the Bight (Lutjeharms et al., 2000), it is assumed that all areas are case 1 unless indicated otherwise by the trigger. Algal1 would be chosen as the default “background” Chl-a product based on previous discussion. The “overlay” would be used in areas where Algal1 has been known to fail, such as sediment dominated and scattering waters; the C2R chlorophyll product would be selected for Chl-a retrieval in these areas. The confidence flag for Algal1 (PCD15) was set as the trigger, as it represents a synthesis of flags for sediment dominated waters, anomalous scattering waters as well as possible areas where atmospheric correction could fail.

The FLH product was used as a verification of the efficacy of the switching algorithm. It should be noted that the relationship between the Chl-a and FLH products has not been specifically validated for the KwaZulu-Natal Bight. Studies have found a strong linear relationship between Chl-a and the FLH computed from the MERIS bands in oligotrophic waters (Gons et al., 2008); however this relationship is known to fail in waters with Chl-a concentrations of more than 20 mg m^{-3} (Gower & King, 2007), where the FLH signal diminishes and becomes negative. Thus the FLH signal was only applied in this study in conjunction with other products, as a qualitative indicator of Chl-a presence in relatively low Chl-a waters; overall spatial consistency between these products tends to give credence to them. Folkestad et al. (2007) also highlighted the usefulness of interpreting the various available Chl-a products together with the additional information provided by CDOM and TSM products, as well as the science and confidence flags. This leads to a more comprehensive understanding of the atmospheric and in-water conditions, and enables an informed evaluation of the reliability of the Chl-a products in a regional context.

The comparisons between the switching algorithm and FLH images in Fig. 4 indicated that there was good synoptic coherency between the two products. Although the FLH product does not quantitatively confirm the accuracy of the switching algorithm, it did reflect most of the variability in the Chl-a concentrations and reduces potential ambiguity in the chlorophyll products (e.g. where high suspended sediment concentrations could be mistaken for high plankton biomass). The linear transect plots (Fig. 4e and f) show coastal Algal1 values more than three times that of C2R; the Algal1 algorithm also appears to fail just off the coast on the 27th of May 2004. The questionable Algal1 values along the coast reinforce the need for case 2 atmospheric correction and marine algorithms in these waters.

A problem with such switching algorithms is generally that, even though the in-water transition between case 1 and case 2 waters is smooth, a sudden switch in algorithms may cause visual artefacts in the water-leaving reflectance images (Brockmann, 2006). This is known as a “hard” classification scheme and can result in uneven or discontinuous retrievals (IOCCG, 2009) as seen in the offshore regions of the Fig. 4c. However, even though there are some inconsistencies in the Chl retrieval, it does, in most cases, not decrease the user's ability to interpret the images. Although visually flawless imagery are considered desirable by users, geophysical returns with a known accuracy and precision on a per-pixel basis should be the first priority.

Ocean colour imagery of the KwaZulu-Natal Bight often indicates areas of increased Chl-a concentration in specific regions of the Bight. These are typically seen as bands of increased Chl-a along the coast, cyclonic eddies in the offshore region and filaments of high Chl-a on the inshore edge of the Agulhas Current. Both examples in Fig. 4 show, to some degree, higher concentrations of Chl-a along the northern coast of the KwaZulu-Natal Bight, most likely as a result of the topographically induced upwelling that occurs in this area (Meyer et al., 2002). Fig. 4d shows an example of tongues of increased Chl-a concentrations that curl southwards at the inner edge of the Agulhas Current, where these upwelled nutrients are dragged along by the current. Elevated riverine influxes also appear to enhance productivity in the inshore zone, as seen in Fig. 4b and d, where tongues of increased Chl-a extend offshore from the Mgeni and Umkomazi rivers in the southern regions of the Bight and the Tugela river in the central region of the Bight. Enhanced Chl-a and nutrient concentrations attributed to rivers have mostly been recorded during flood events at the Tugela river mouth (Carter & Schleyer, 1988).

Please cite this article as: Smith, M.E., et al., The assessment of optimal MERIS ocean colour products in the shelf waters of the KwaZulu-Natal Bight, South Africa, *Remote Sensing of Environment* (2013), http://dx.doi.org/10.1016/j.rse.2013.06.009

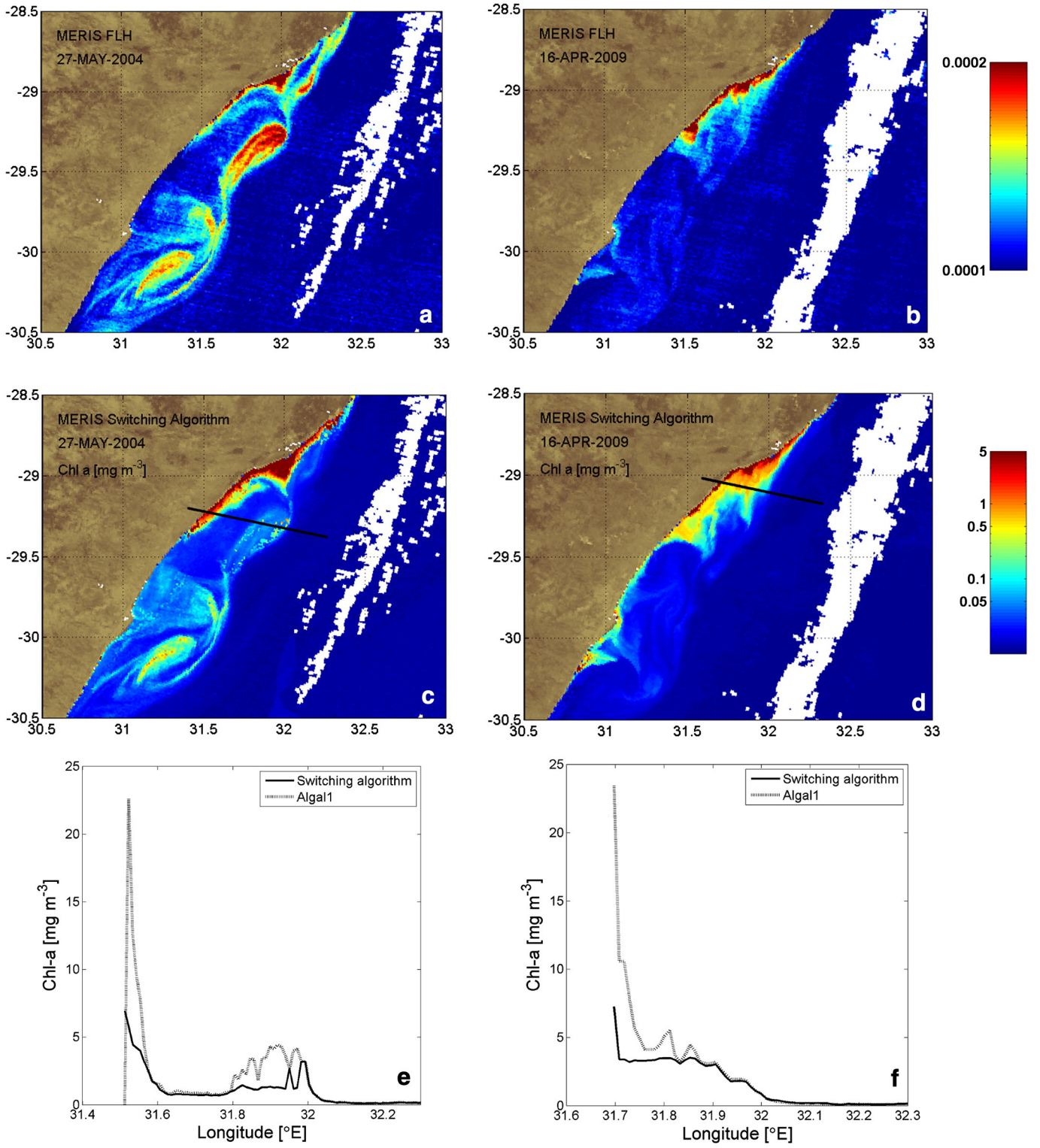

Fig. 4. Images of fluorescence line height (a & b) and the switching algorithm (c & d). Images on the left represent the 27th May 2004, whilst images on the right show 16th April 2009. Linear transect plots (e) and (f) show results of the Algal1 and Switching algorithm Chl-a concentrations as represented by the lines in images (c) and (d) respectively.

Occasionally, cyclonic recirculation features occur in the outer Bight waters at the inshore edge of the Agulhas Current. These are most likely lee eddies (Pearce, Schumann, & Lundie, 1978) formed as a result of the passing current. The entrainment and dynamic retention of nutrients in the surface waters of these eddies could enhance the growth of phytoplankton as seen in Fig. 4a and c. During Natal Pulse events these eddies can have diameter ranges of between 30 and 200 km (De Ruijter, van Leeuwen, & Lutjeharms, 1999), resulting in high Chl-a concentrations occurring further offshore than usual.

The examination of the causal factors of specific events of increased productivity could potentially be aided with the use of additional ocean colour products; slight increases in the offshore concentrations of TSM and CDOM could indicate the entrainment and recirculation of riverine waters by eddies, whilst the additional use of sea surface temperature

Please cite this article as: Smith, M.E., et al., The assessment of optimal MERIS ocean colour products in the shelf waters of the KwaZulu-Natal Bight, South Africa, *Remote Sensing of Environment* (2013), http://dx.doi.org/10.1016/j.rse.2013.06.009

data could serve as an indication to the extent and influence of upwelling. The switching algorithm could therefore facilitate the observation of the event scale drivers in the KwaZulu-Natal Bight and Agulhas systems with the least amount of data lost to turbid waters or atmospheric correction problems. When implemented together with the flags and the FLH, TSM and CDOM products, the user could potentially achieve a widespread understanding of the biogeochemical and bio-optical system function.

6. Conclusion

This study presents an initial evaluation of the performance of MERIS ocean colour algorithms in the KwaZulu-Natal Bight, with particular focus on the reflectance and chlorophyll products from the C2R, 2nd and 3rd reprocessing. It should be mentioned that the results given in this study represent only a snapshot of the potential bio-optical conditions that may occur in the waters of the KwaZulu-Natal Bight. As the first radiometric and water constituent assessment to be performed in the area, this study provides a foundation for further work and represents only an indication of the MERIS products that could be optimal for use in the area.

The variability in the bio-optical nature of the system has been highlighted and emphasizes the need for an adaptable method when using ocean colour remote sensing as a routine observational monitoring platform for the Bight waters. Algal1 from MEGS v8.0 gave good results in case 1 waters, whilst the C2R Chl-a product was chosen as a temporary case 2 product until further validation can be performed. A switching algorithm was presented which triggers on the PCD15 confidence flag. The new algorithm's efficacy has been demonstrated with its qualitative similarities to the FLH product. When used together with the other available MERIS products and flags, it aids the observation of event scale drivers, forcing mechanisms and functioning of the KwaZulu-Natal Bight and Agulhas systems.

It is recommended that future radiometric and biogeochemical validation exercises be performed at the Tugela River mouth region, preferably during times of high riverine output. These should include measurements of CDOM and SPM, which would facilitate the assessment of marine and atmospheric case 2 algorithms in a more complex bio-optical environment. It is further recommended that future studies in the area endeavour to use full resolution satellite data whenever possible, since this can reduce the errors introduced by the difference in spatial resolution when comparing an in situ measurement to a satellite pixel.

The CoastColour project facilitates inter-comparison and validation of various case 2 algorithms over globally distributed coastal sites focus specifically on the use of full resolution MERIS data. These data include improved atmospheric correction, as well as regional case 2 water algorithms; consequently CoastColour products could also prove useful in the KwaZulu-Natal Bight region and should be considered for future ocean colour product assessments in the region.

A valuable expansion on the switching algorithm concept would be the development of a dynamic classification scheme (IOCCG, 2009). This approach operates by classifying waters based on their spectral reflectance characteristics and bio-optical signatures (e.g. Lubac & Loisel, 2007; Martin Traykovski & Sosik, 2003; Moore, Campbell, & Feng, 2001); the appropriate algorithms for each water class can then be applied with the use of fuzzy logic (IOCCG, 2009) which blends products in order to avoid the spatial discontinuities that occur when using hard classification schemes. Due to its variable bio-optical nature, the KwaZulu-Natal Bight would be a prime example for the application of dynamic classification schemes. Future studies could also consider the application of non sensor-specific empirical case 2 algorithms (e.g. Gietelson, Gurlin, Moses, & Barrow, 2009), or possibly even create new local analytical algorithms specific for the KwaZulu-Natal Bight waters, like those produced by Bernard et al. (2005) for the Benguela.

In terms of long-term monitoring of the KwaZulu-Natal Bight system: future ESA missions include the ocean and land colour instrument (OLCI) on board the Sentinel-3 satellite which is scheduled to launch in 2014. This would be the follow-up to MERIS and will include similar spectral bands, swath and spectral coverage. Future algorithms could be designed for application with this instrument.

Currently there is little ocean colour validation activity in African shelf environments. The KwaZulu-Natal Bight bio-optical conditions are similar to that of the east coast of Africa, with inshore areas affected by riverine influxes that changes to offshore oligotrophic conditions over a relatively small spatial scale. The switching algorithm could therefore be a suitable first order product in these areas. It offers ease of implementation since it is based on existing MERIS products and the operational application is possible with established processing chains and dissemination facilities. Switching algorithm products can therefore be routinely disseminated to East African users, and are likely to offer a starting point until validation data become available for these areas.

7. Uncited reference

Santer and Zagolski, 2008

Acknowledgements

Thanks to ACCESS, CSIR, MA-RE, University of Cape Town Postgraduate Publication Incentive Scholarship, the START (Global change system for analysis, research, and training) programme, WRC and Frank Shillington for the funding and bursaries that they provided. For the use of their laboratory and/or equipment we wish to thank Dr AJ Smith from UKZN, Grant Pitcher and Trevor Probyn from DAFF, and Isabelle Ansorge and Howard Waldron from UCT. Thanks to Rhyn and John Harding for skippering and help with data collection. The MERIS data were made available by the European Space Agency.

References

Aiken, J., Fishwick, J. R., Lavender, S., Barlow, R., Moore, G. F., Sessions, H., et al. (2007). Validation of MERIS reflectance and chlorophyll during the BENCAL cruise October 2002: Preliminary validation of new demonstration products for phytoplankton functional types and photosynthetic parameters. *International Journal of Remote Sensing, 28*(3), 497–516.

Aiken, J., & Moore, G. (2000). *Case 2 (S) bright pixel atmospheric correction, MERIS ATBD 2.6.* Plymouth: Plymouth Marine Laboratory.

Ambarwulan, W., Mannaerts, C. M., van der Woerd, H. J., & Salama, Mhd. S. (2010). Medium resolution imaging spectrometer data for monitoring tropical coastal waters: A case study of Berau estuary, East Kalimantan, Indonesia. *Geocarto International, 25*(7), 525–541.

Ångström, A. (1964). The parameters of atmospheric turbidity. *Tellus, 16*, 64–75.

Antoine, D., Chami, M., Claustre, H., D'Ortenzio, F., Morel, A., Bécu, G., et al. (2006). *BOUSSOLE: A joint CNRS-INSU, ESA, CNES and NASA ocean color calibration and validation activity.* NASA technical memorandum, No. TM-2006-214147. Greenbelt, USA: NASA/GSFC.

Antoine, D., d'Ortenzio, F., Hooker, S. B., Bécu, G., Gentili, B., Tailliez, D., et al. (2008). Assessment of uncertainty in the ocean reflectance determined by three satellite ocean color sensors (MERIS, SeaWiFS and MODIS-A) at an offshore site in the Mediterranean Sea (BOUSSOLE project). *Journal of Geophysical Research, 113*, C07013. http://dx.doi.org/10.1029/2007JC004472.

Antoine, D., & Morel, A. (2005). *Atmospheric correction of the MERIS observations over ocean case 1 waters.* MERIS ATBD 2.7. Laboratoire d'Oceanographie de Villefranche (Issue 5, Revision 0).

Antoine, D., & Morel, A. (2011). *Atmospheric correction of the MERIS observations over ocean case 1 waters.* MERIS ATBD 2.7. Laboratoire d'Oceanographie de Villefranche (Issue 5, Revision 1).

Babin, M., Morel, A., Fournier-Sicre, V., Fell, F., & Stramski, D. (2003). Light scattering properties of marine particles in coastal and open waters as related to the particle mass concentration. *Limnology and Oceanography, 48*(2), 843–859.

Babin, M., Morel, A., & Gentili, B. (1996). Remote sensing of sea surface sun-induced chlorophyll fluorescence: Consequences of natural variations in the optical characteristics of phytoplankton and the quantum yield of chlorophyll a fluorescence. *International Journal of Remote Sensing, 17*(12), 2417–2448.

Please cite this article as: Smith, M.E., et al., The assessment of optimal MERIS ocean colour products in the shelf waters of the KwaZulu-Natal Bight, South Africa, *Remote Sensing of Environment* (2013), http://dx.doi.org/10.1016/j.rse.2013.06.009

Balch, W. M., Kilpatrick, K. A., Holligan, P., & Fernandez, E. (1996). The 1991 coccolithophore bloom in the central north Atlantic. 2. Relating optics to coccolith concentration. *Limnology and Oceanography*, *41*(8), 1684–1696.

Bernard, S., Balt, C., Pitcher, G., Probyn, T., Fawcett, A., & Du Randt, A. (2005). The use of MERIS for harmful algal bloom monitoring in the Southern Benguela. In ESA/ESRIN (Ed.), *Proceedings of the MERIS/(A)ATSR Workshop, Frascati, Italy*.

Bernard, S., Kudela, R. M., Franks, P., Fennel, W., Kemp, A., Fawcett, A., et al. (2006). The requirements for forecasting harmful algal blooms in the Benguela. *The Benguela: Predicting a large marine ecosystem*. In V. Shannon, G. Hempel, P. Malanotte-Rizzoli, C. Moloney, & J. Woods (Eds.), *Large marine ecosystems*, *14*. (pp. 273–294). Elsevier.

Bianchi, T. S., Lambert, C., & Biggs, D. C. (1995). Distribution of chlorophyll *a* and phaeopigments in the northwestern Gulf of Mexico: a comparison between fluorometric and High-Performance Liquid Chromatography measurements. *Bulletin of Marine Science*, *56*(1), 25–32.

Binding, C. E., Greenberg, T. A., Jerome, J. H., Bukata, R. P., & Letourneau, G. (2011). An assessment of MERIS algal products during an intense bloom in Lake of the Woods. *Journal of Plankton Research*, *33*, 793–806.

Blondeau-Patissier, D., Tilstone, G. H., Martinez-Vicente, V., & Moore, G. F. (2004). Comparison of bio-physical marine products from SeaWiFS, MODIS and a bio-optical model with in situ measurements from Northern European waters. *Journal of Optics A: Pure and Applied Optics*, *6*, 875–889.

Boss, E., & Zaneveld, J. R. V. (2003). The effect of bottom substrate on inherent optical properties: Evidence of biogeochemical processes. *Limnology and Oceanography*, *48*(1, part 2), 346–354.

Bourg, L., & Members of the MERIS Quality Working Group (2012). *MERIS 3rd data reprocessing: Validation report*. European Space Agency Report. Ref A879-NT-017-ACR.

Bowers, D. G., Evans, D., Thomas, D. N., Ellis, K., & Williams, P. J. le B. (2004). Interpreting the colour of an estuary. *Estuarine, Coastal and Shelf Science*, *59*, 13–20.

Bowers, D. G., Harker, G. E. L., Smith, P. S. D., & Tett, P. (2000). Optical properties of a region of freshwater influence (the Clyde Sea). *Estuarine, Coastal and Shelf Science*, *50*, 717–726.

Bricaud, A., Morel, A., & Prieur, L. (1981). Absorption by dissolved organic matter of the sea (yellow substance) in the UV and visible domains. *Limnology and Oceanography*, *26*(1), 43–53.

Brockmann, C. (2006). Limitations of the application of the MERIS atmospheric correction. In ESA/ESRIN (Ed.), *Proceedings of the Second Working Meeting on MERIS and AATSR Calibration and Geophysical Validation. Frascati, Italy*.

Carter, R. A., & d'Aubrey, J. (1988). Inorganic nutrients in Natal continental shelf waters. *Coastal ocean studies off Natal, South Africa*. In E. H. Schumann (Ed.), *Lecture notes on coastal and estuarine studies*, *26*. (pp. 131–151). Berlin: Springer.

Carter, R. A., & Schleyer, M. H. (1988). Plankton distributions in Natal coastal waters. *Coastal ocean studies off Natal, South Africa*. In E. H. Schumann (Ed.), *Lecture notes on coastal and estuarine studies*, *26*. (pp. 152–177). Berlin: Springer.

Cox, C., & Munk, W. (1954). The measurements of the roughness of the sea surface from photographs of the sun's glitter. *Journal of the Optical Society of America*, *44*, 838–850.

Cristina, S. V., Goela, P., Icely, J. D., Newton, A., & Fragoso, B. (2009). Assessment of water-leaving reflectance of oceanic and coastal waters using MERIS satellite products off the southwest coast of Portugal. *Journal of Coastal Research*, *56*, 1479–1483.

Cui, T., Zhang, J., Groom, S., Sun, L., Smyth, T., & Sathyendranath, S. (2010). Validation of MERIS ocean-color products in the Bohai Sea: A case study for turbid coastal waters. *Remote Sensing of Environment*, *114*, 2326–2336.

Darecki, M., & Stramski, D. (2004). An evaluation of MODIS and SeaWiFS bio-optical algorithms in the Baltic Sea. *Remote Sensing of Environment*, *89*, 326–350.

De Ruijter, W. P. M., van Leeuwen, P. J., & Lutjeharms, J. R. E. (1999). Generation and evolution of Natal Pulses: Solitary meanders in the Agulhas Current. *Journal of Physical Oceanography*, *29*, 3043–3055.

Doerffer, R. (2011). *Alternative atmospheric correction procedure for Case 2 water remote sensing using MERIS (ATBD)*. Helmholtz-Zentrum, No. 1.0. Geesthacht.

Doerffer, R., & Schiller, H. (2006). *MERIS advanced water algorithm, atmospheric correction algorithm theoretical basis document (ATBD)*. GKSS Research Centre, No. 1.1. Geesthacht.

Doerffer, R., & Schiller, H. (2007). The MERIS Case 2 water algorithm. *International Journal of Remote Sensing*, *28*, 517–535.

Doerffer, R., & Schiller, H. (2008a). *MERIS regional coastal and lake Case 2 water project — atmospheric correction Algorithm Theoretical Basis Document (ATBD)*. GKSS Research Centre, No. 1.0. Geesthacht.

Doerffer, R., & Schiller, H. (2008b). *MERIS lake water algorithm for BEAM algorithm theoretical basis document (ATBD)*. GKSS Forschungszentrum, No. 1.0. Geesthacht.

Dzwonkowski, B., & Yan, X. -H. (2005). Tracking of a Chesapeake Bay estuarine outflow plume with satellite-based ocean color data. *Continental Shelf Research*, *25*, 1942–1958.

Folkestad, A., Pettersson, L. H., & Durand, D. D. (2007). Inter-comparison of ocean colour data products during algal blooms in the Skagerrak. *International Journal of Remote Sensing*, *28*(3–4), 569–592.

Gietelson, A. A., Gurlin, D., Moses, W. J., & Barrow, T. (2009). A bio-optical algorithm for the remote estimation of the chlorophyll-a concentration in case 2 waters. *Environmental Research Letters*, *4*, 045003. http://dx.doi.org/10.1088/1748-9326/4/4/045003.

Gons, H. J., Auer, M. T., & Effler, S. W. (2008). MERIS satellite chlorophyll mapping of oligotrophic and eutrophic waters in the Laurentian Great Lakes. *Remote Sensing of Environment*, *112*, 4098–4106.

Gordon, H. R. (1992). Diffuse reflectance of the ocean: influence of nonuniform phytoplankton pigment profile. *Applied Optics*, *31*(12), 2116–2129.

Gordon, H. R., & Clarke, D. K. (1980). Remote sensing optical properties of a stratified ocean: an improved interpretation. *Applied Optics*, *19*(20), 3428–3430.

Gordon, H. R., & McCluney, W. R. (1975). Estimation of the depth of sunlight penetration in the sea for remote sensing. *Applied Optics*, *14*(2), 413–416.

Gordon, H. R., & Morel, A. (1983). Remote assessment of ocean color for interpretation of satellite visible imagery: A review. *Lecture notes on coastal and estuarine studies*, *Vol. 4*, New York: Springer Verlag.

Gower, J. F. R., Doerffer, R., & Borstad, G. A. (1999). Interpretation of the 685 nm peak in water-leaving radiance spectra in terms of fluorescence, absorption and scattering, and its observation by MERIS. *International Journal of Remote Sensing*, *20*(9), 1771–1786.

Gower, J. F. R., & King, S. (2007). Validation of chlorophyll fluorescence derived from MERIS on the west coast of Canada. *International Journal of Remote Sensing*, *28*(3–4), 625–635.

Hirawake, T., Kudoh, S., Aoki, S., & Rintoul, S. R. (2003). Eddies revealed by SeaWiFS ocean color images in the Antarctic Divergence zone near 140°E. *Geophysical Research Letters*, *30*(9), 1458. http://dx.doi.org/10.1029/2003GL016996.

Holm-Hansen, O., Kahru, M., Hewes, C. D., Kawaguchi, S., Kameda, T., Sushin, V. A., et al. (2004). Temporal and spatial distribution of chlorophyll- a in surface waters of the Scotia Sea as determined by both shipboard measurements and satellite data. *Deep-Sea Research II*, *51*, 1323–1331.

Holm-Hansen, O., Lorenzen, C. J., Holmes, R. W., & Strickland, J. D. H. (1965). Fluorometric determination of chlorophyll. *Journal du Conseil*, *30*, 3–15.

Hu, C., Lee, Z., Muller-Karger, F. E., & Carder, K. L. (2003). Application of an optimization algorithm to satellite ocean color imagery: A case study in Southwest Florida coastal waters. In R. J. Frouin, Y. Yuan, & H. Kawamura (Eds.), *SPIE Proceedings: Ocean Remote Sensing and Applications*, *4892*. (pp. 70–79)Bellingham, WA: SPIE.

Hu, C. M., Luerssen, R., Muller-Karger, E. F., Carder, L. K., & Heil, A. C. (2008). On the remote monitoring of *Karenia brevis* blooms of the west Florida shelf. *Continental Shelf Research*, *28*, 159–176.

Hu, C., Montgomery, E. T., Schmitt, R. W., & Muller-Karger, F. E. (2004). The dispersal of the Amazon and Orinoco River water in the tropical Atlantic and Caribbean Sea: Observation from space and S-PALACE floats. *Deep-Sea Research II*, *51*, 1151–1171.

Hutchings, L., Beckley, L. E., Griffiths, M. H., Roberts, M. J., Sundby, S., & van der Lingen, C. (2002). Spawning on the edge: Spawning grounds and nursery areas around the southern African coastline. *Marine and Freshwater Research*, *53*(2), 307–318.

IOCCG (2009). Partition of the ocean into ecological provinces: Role of ocean-colour radiometry. In M. Dowell, & T. Platt (Eds.), *Reports of the International Ocean-Colour Coordinating Group, No. 9, IOCCG, Dartmouth, Canada*.

Kratzer, S., Brockmann, C., & Moore, G. (2008). Using MERIS full resolution data to monitor coastal waters — A case study from Himmerfjarden, a fjord-like bay in the northwestern Baltic Sea. *Remote Sensing of Environment*, *112*, 2284–2300.

Kutchinke, C. P., Gordon, H. R., & Franz, B. A. (2009). Spectral optimization for constituent retrieval in Case 2 waters I: Implementation and performance. *Remote Sensing of Environment*, *113*, 571–587.

Kutser, T. (2004). Quantitative detection of chlorophyll in cyanobacterial blooms by satellite remote sensing. *Limnology and Oceanography*, *49*(6), 2,179–2,189.

Leathers, R. A., Downes, T. V., & Mobley, C. D. (2001). Self-shading correction for upwelling sea-surface radiance measurements made with buoyed instruments. *Optics Express*, *8*(10), 561–570.

Lerebourg, C., & Bruniquel, V. (2011). *MERIS 3rd data reprocessing software and ADF updates*. European Space Agency Report. Ref, A879.NT.008.ACRI-ST.

Loisel, H., & Morel, A. (1998). Light scattering and chlorophyll concentration in case 1 waters: A re-examination. *Limnology and Oceanography*, *43*(5), 847–858.

Lubac, B., & Loisel, H. (2007). Variability and classification of remote sensing reflectance spectra in the eastern English Channel and southern North Sea. *Remote Sensing of Environment*, *110*, 45–58.

Lutjeharms, J. R. E., Valentine, H. R., & Van Ballegooyen, R. C. (2000). The hydrography and water masses of the Natal Bight, South Africa. *Continental Shelf Research*, *20*, 1907–1939.

Maffioni, R. A., & Dana, D. R. (1997). Instruments and methods for measuring the backward-scattering coefficient of ocean waters. *Applied Optics*, *36*(24), 6057–6067.

Maritorena, S., Siegel, D. A., & Peterson, A. R. (2002). Optimization of a semianalytical ocean color model for global-scale applications. *Applied Optics*, *41*(15), 2705–2714.

Martin Traykovski, L. V., & Sosik, H. M. (2003). Feature-based classification of optical water types in the Northwest Atlantic based on satellite ocean color data. *Journal of Geophysical Research*, *108*(C5), 3150. http://dx.doi.org/10.1029/2001JC001172.

Matthews, M. W., Bernard, S., & Winter, K. (2010). Remote sensing of cyanobacteria-dominant algal blooms and water quality parameters in Zeekoevlei, a small hypertrophic lake, using MERIS. *Remote Sensing of Environment*, *114*(1), 106–115.

Meyer, A. A., Lutjeharms, J. R. E., & de Villiers, S. (2002). The nutrient characteristics of the Natal Bight, South Africa. *Journal of Marine Systems*, *35*, 11–37.

Mobley, C. D. (1994). *Light and water: Radiative transfer in natural waters*. San Diego: Academic Press.

Mobley, C. D., Gentili, B., Gordon, H. R., Jin, Z., Kattawar, G. W., Morel, A., et al. (1993). Comparison of numerical models for computing underwater light fields. *Applied Optics*, *32*(36), 7484–7505.

Mobley, C. D., Stramski, D., Bissett, W. P., & Boss, E. (2004). Optical modeling of ocean waters: Is the Case 1–Case 2 classification still useful? *Oceanography*, *17*(2), 61–67.

Molleri, G. S. F., deM Novo, E. M. L., & Kampel, M. (2010). Space–time variability of the Amazon River plume based on satellite ocean color. *Continental Shelf Research*, *30*, 342–352.

Moore, T. S., Campbell, J. W., & Feng, H. (2001). A fuzzy logic classification scheme for selecting and blending satellite ocean colour algorithms. *IEEE Transactions on Geoscience and Remote Sensing*, *39*, 1764–1776.

Moore, G., & Lavender, S. (2011). *MERIS ATBD 2.6 — CaseII.S bright pixel atmospheric correction*. Bio Optica ARGANS, No. 5.0.

Please cite this article as: Smith, M.E., et al., The assessment of optimal MERIS ocean colour products in the shelf waters of the KwaZulu-Natal Bight, South Africa, *Remote Sensing of Environment* (2013), http://dx.doi.org/10.1016/j.rse.2013.06.009

Morel, A. (1974). Optical properties of pure water and pure sea water. In N. G. Jerlov, & E. S. Nielsen (Eds.), *Optical aspects of oceanography* (pp. 1–24). New York: Academic Press.

Morel, A. (1988). Optical modeling of the upper ocean in relation to its biogenous matter content (Case 1 water). *Journal of Geophysical Research*, *93*(10), 749–768.

Morel, A., & Antoine, D. (2007). *MERIS ATBD 2.9 — Pigment index retrieval in Case 1 waters.* Laboratoire d'Océanographie de Villefranche, No. 4.2. Villefranche.

Morel, A., & Antoine, D. (2011). *MERIS ATBD 2.9 — Pigment index retrieval in Case 1 waters.* Laboratoire d'Océanographie de Villefranche, No. 4.3. Villefranche.

Morel, A., Huot, Y., Gentili, B., Werdell, P. J., Hooker, S. B., & Franz, B. A. (2007). Examining the consistency of products derived from various ocean color sensors in open ocean (Case 1) waters in the perspective of a multi-sensor approach. *Remote Sensing of Environment*, *111*, 69–88.

Morel, A., & Maritorena, S. (2001). Bio-optical properties of oceanic waters: A reappraisal. *Journal of Geophysical Research*, *106*(C4), 7163–7180.

Morel, A., & Prieur, L. (1977). Analysis of variations in ocean colour. *Limnology and Oceanography*, *22*(4), 709–722.

Odermatt, D., Giardino, C., & Heege, T. (2010). Chlorophyll retrieval with MERIS Case-2-Regional in perialpine lakes. *Remote Sensing of Environment*, *114*, 607–617.

Ohde, T., Siegel, H., & Gerth, M. (2007). Validation of MERIS Level-2 products in the Baltic Sea, the Namibian coastal area and the Atlantic Ocean. *International Journal of Remote Sensing*, *28*(3–4), 609–624.

O'Reilly, J. E., Maritorena, S., O'Brien, M. C., Siegel, D. A., Toole, D., Menzies, D., et al. (2000). SeaWiFS postlaunch calibration and validation analyses. *NASA Technical Memorandum*, *11*(3) (49 pp.).

Park, Y., Van Mol, B., & Ruddick, K. (2006). Validation of MERIS water products for Belgian coastal waters: 2002–2005. In ESA/ESRIN (Ed.), *Proceedings of the Second Working Meeting on MERIS and (A)ATSR Calibration and Geophysical Validation. Frascati, Italy.*

Pearce, A. F., Schumann, E. H., & Lundie, G. S. H. (1978). Features of the shelf circulation off the Natal coast. *South African Journal of Science*, *74*, 328–331.

Pegau, W. S., Boss, E., & Martinez, A. (2002). Ocean color observations of eddies during the summer in the Gulf of California. *Geophysical Research Letters*, *29*(9). http://dx.doi.org/10.1029/2001GL014076.

Pitcher, G. C., Bernard, S., & Ntuli, J. (2008). Contrasting bays and red tides in the southern Benguela upwelling system. *Oceanography*, *21*(3), 82–91.

Pope, R. M., & Fry, E. S. (1997). Absorption spectrum (380–700 nm) of pure water. II. Integrating cavity measurements. *Applied Optics*, *36*(33), 8710–8723.

Preisendorfer, R. W. (1986). Secchi disk science: Visual optics of natural waters. *Limnology and Oceanography*, *31*(5), 909–926.

Prieur, L., & Sathyendranath, S. (1981). An optical classification of coastal and oceanic waters based on the specific spectral absorption curves of phytolankton pigments, dissolved organic matter, and other particulate materials. *Limnology and Oceanography*, *26*(4), 671–689.

Ruiz-Verdú, A., Koponen, S., Heege, T., Doerffer, R., Brockmann, C., Kallio, K., et al. (2008). Development of MERIS lake water algorithms: Validation results from Europe. In ESA/ESRIN (Ed.), *Proceedings of the 2nd MERIS/(A)ATSR user workshop. Frascati, Italy*.

Ryan, J. P., Fischer, A. M., Kudela, R. M., Gower, J. F. R., King, S. A., Marin, R., III, et al. (2009). Influences of upwelling and downwelling winds on red tide bloom dynamics in Monterey Bay, California. *Continental Shelf Research*, *29*, 785–795.

Santer, R., & Zagolski, F. (2008). *Improve Contrast between Ocean and Land (ICOL): Algorithm Theoretical Basis Document (ATBD): The MERIS Level-1C.* France: Université du Littoral Côte d'Opale, ADRINORD.

Schroeder, T. H., Schaale, M., & Fischer, J. (2007). Retrieval of atmospheric and oceanic properties from MERIS measurements: A new Case-2 water processor for BEAM. *International Journal of Remote Sensing*, *28*(24), 5627–5632.

Smirnov, A., Holben, B. N., Giles, D. M., Slutsker, I., O'Neill, N. T., Eck, T. F., et al. (2011). Maritime aerosol network as a component of AERONET — First results and comparison with global aerosol models and satellite retrievals. *Atmospheric Measurement Techniques Discussions*, *4*, 583–597. http://dx.doi.org/10.5194/amt-4-583-2011.

Sørensen, K., Aas, E., & Høkedal, J. (2007). Validation of MERIS water products and bio-optical relationships in the Skagerrak. *International Journal of Remote Sensing*, *28*(3–4), 555–568.

Takashima, T., & Masuda, K. (2000). Atmospheric correction for the satellite visible data over heterogeneous surfaces. *Applied Mathematics and Computation*, *116*, 181–196.

Theis, A., Schmitt, B., Gehnke, S., Doerffer, R., & Bracher, A. (2008). Validation of MERIS remote sensing reflectance in Atlantic Case 1 waters with ground based in-situ measurements. In ESA/ESRIN (Ed.), *Proceedings of the 2nd MERIS/(A)ATSR user workshop. Frascati, Italy*.

Toledano, C., Cachorro, V. E., Berjon, A., de Frutos, A. M., Sorribas, M., de la Morena, B. A., et al. (2007). Aerosol optical depth and Ångström exponent climatology at El Arenosillo AERONET site (Huelva, Spain). *The Quarterly Journal of the Royal Meteorological Society*, *133*, 795–807.

Trees, C. C., Kennicutt, M. C., II, & Brooks, J. M. (1985). Errors associated with the standard fluorometric determination of chlorophylls and phaeopigment. *Marine Chemistry*, *17*(1), 1–12.

Werdell, P. J., Bailey, S. W., Franz, B. A., Harding, L. W., Jr., Feldman, G. C., & McClain, C. R. (2009). Regional and seasonal variability of chlorophyll-a in Chesapeake Bay as observed by SeaWiFS and MODIS-Aqua. *Remote Sensing of Environment*, *113*, 1319–1330.

Xing, P., Kong, F. X., Cao, H. S., Zhang, M., & Tan, X. (2007). Variations of bacterioplankton community composition during *Microcystis* spp. blooms in a shallow eutrophic lake. *Journal of Freshwater Ecology*, *22*(1), 61–67.

Zibordi, G., Berthon, J. -F., Mélin, F., & D'Alimonte, D. (2011). Cross-site consistent in situ measurements for satellite ocean color applications: The BiOMaP radiometric dataset. *Remote Sensing of Environment*, *115*, 2104–2115.

Zibordi, G., Mélin, F., & Berthon, J. -F. (2006). Comparison of SeaWiFS, MODIS and MERIS radiometric products at a coastal site. *Geophysical Research Letters*, *33*, L06617. http://dx.doi.org/10.1029/2006GL025778.

Please cite this article as: Smith, M.E., et al., The assessment of optimal MERIS ocean colour products in the shelf waters of the KwaZulu-Natal Bight, South Africa, *Remote Sensing of Environment* (2013), http://dx.doi.org/10.1016/j.rse.2013.06.009